Expression of a Full-Length Hepatitis C Virus cDNA Up-Regulates the Expression of CC Chemokines MCP-1 and RANTES

Hui Meng Soo,* Alfredo Garzino-Demo,† Wanjin Hong,‡ Yin Hwee Tan,* Yee Joo Tan,*
Phuay-Yee Goh,* Seng Gee Lim,§ and Siew Pheng Lim*,[1]

*Collaborative Anti-Viral Research Laboratory, and ‡Membrane Biology Laboratory, Institute of Molecular and Cell Biology, 30 Medical Drive, Singapore 117609; †Institute of Human Virology, University of Maryland Biotechnology Institute, Baltimore, Maryland 21201; and §Department of Medicine, National University Hospital, 5 Lower Kent Ridge Road, Singapore 119074

We had previously reported the cloning of the complete genome of an isolate of hepatitis C virus (HCV), HCV-S1, of genotype 1b. We have constructed a full-length complementary DNA (cDNA) clone of HCV-S1 using nine overlapping cDNA clones that encompassed its entire genome. HCV core, E1, E2, NS-3, -4B, -5A, and -5B proteins were detected in 293T cells by immunoblot analyses when expression of the full-length HCV-S1 was driven under a CMV promoter. Expression of full-length HCV-S1 led to induction of the CC chemokines RANTES and MCP-1 at both the mRNA and the protein levels in HeLa, Huh7, and HepG2 cells. Reporter gene assays showed that a minimal MCP-1 promoter construct containing 128 nucleotides upstream of its translational start site was sufficient for optimal HCV-mediated activation. HCV induced AP-1 binding activities to this region, as determined from electrophoretic mobility shift assays and supershifts with anti-AP-1 antibodies. Transfection of full-length HCV-S1 up-regulated both AP-1 binding activities as well as c-*jun* transcripts. A minimal promoter construct containing 181 nucleotides upstream of the RANTES translational start site was sufficient for maximal HCV-mediated induction. Gel mobility shift and supershift assays showed that HCV induced NF-κB and other unknown binding activities to the A/B-site within this region. In HeLa cells, HCV core and NS5A could separately augment promoter activities of both MCP-1 and RANTES. In Huh7 cells, only NS5A produced a similar effect, while rather surprisingly, HCV core induced a dramatic reduction in promoter activities of these two genes. This study provides the first direct evidence for the induction of CC chemokines in HCV infection and draws attention to their roles in affecting the progress and outcome of HCV-associated liver diseases. © 2002 Elsevier Science (USA)

Key Words: full-length; hepatitis C virus; induce; expression; chemokine; RANTES; MCP-1; RNA; protein; pathogenesis.

INTRODUCTION

Hepatitis C virus (HCV) is a member of the *Flaviviridae* family, and the major cause of chronic liver disease worldwide (Alter *et al.,* 1989; Houghton *et al.,* 1991). HCV is an enveloped virus with a single-stranded, positive-sense, nonsegmented RNA genome that encodes a single open reading frame (ORF) of 3010 amino acids (aa), which is cotranslationally and posttranslationally cleaved to give at least 10 polypeptides (Choo *et al.,* 1991). Located at its N-terminal end are three structural proteins, followed by at least seven nonstructural (NS) proteins (Choo *et al.,* 1991). These proteins are processed by a host-derived signalase and cleaved by virus-encoded proteases (Harada *et al.,* 1991; Hijikata *et al.,* 1991; Matsura *et al.,* 1992; Selby *et al.,* 1993; Tomei *et al.,* 1993).

Similar to other RNA viruses, the genome of HCV is highly heterogeneous, and several genotypes and subtypes have been described (Lanford *et al.,* 1994; Ito *et al.,*

1996). Numerous studies have successfully demonstrated partial replication of the virus in *in vitro* culture systems using human T and B cells (Bertolini *et al.,* 1993; Shimizu *et al.,* 1993) and hepatocytes of human (Iacovacci *et al.,* 1993; Ito *et al.,* 1996; Ikeda *et al.,* 1998) or chimpanzee origin (Lanford *et al.,* 1994). However, these systems suffer from low viral replication efficiency and limited passage cycles. More recently, high-level replication of subgenomic HCV RNAs was established in a human hepatoma cell line that would enable long-term production of viral RNAs and proteins (Lohmann *et al.,* 1999; Blight *et al.,* 2000).

Thus the steps taken to construct a full-length HCV clone are of paramount importance in determining its replication-competence and infectivity. Nucleotide sequences have been reported for at least 42 HCV genomes from around the world. However, several of these sequences were derived from pooled plasma samples of HCV-infected patients, with only one or two obtained from infected individuals (Aizaki *et al.,* 1998). To this end, we have taken the path toward creating a replication-competent full-length HCV genome by the assembly of overlapping cDNA clones derived from a thalessemia

[1] To whom correspondence and reprint requests should be addressed. Fax: (65) 779-1117. E-mail: mcblimsp@imcb.nus.edu.sg.
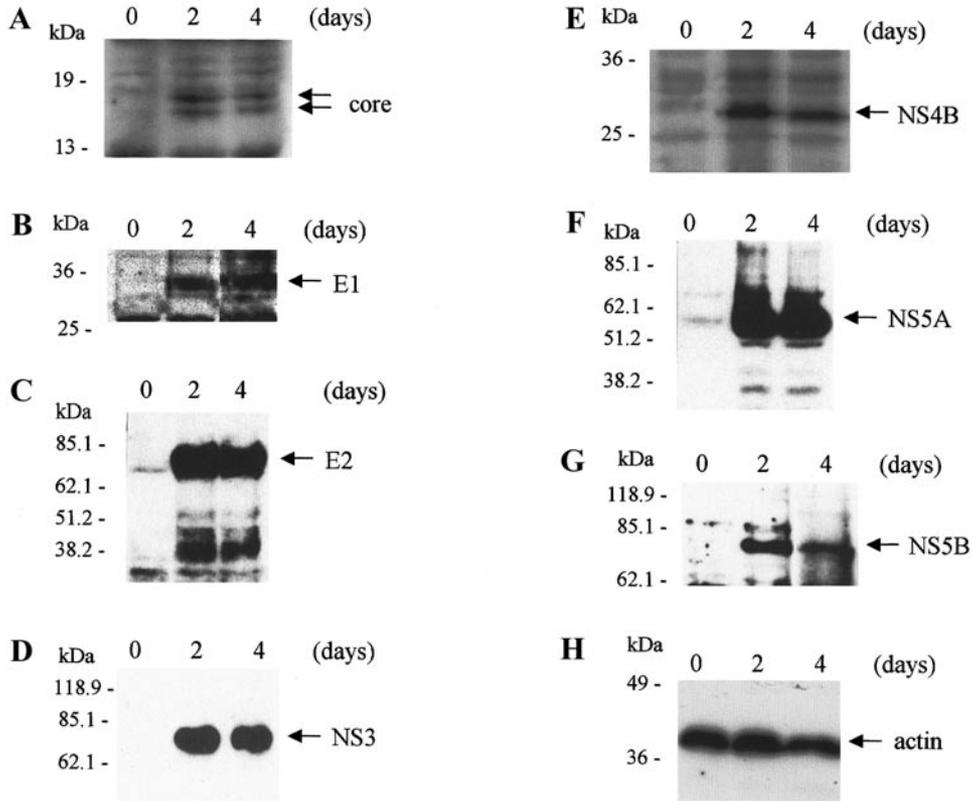
FIG. 1. Expression of HCV structural and nonstructural proteins (A–G) in 293T cells transiently transfected with a full-length (FL) HCV expression construct, pXJ(S1). Cells were harvested at 2 and 4 days posttransfection. Untransfected cells were used as controls (Day 0). Cells were lysed and resolved on 12% SDS–PAGE gels and subjected to immunoblot analyses with the various antibodies as described under Materials and Methods. Arrows indicate the respective HCV proteins. Molecular masses in kilodaltons (kDa) of protein molecular weight markers are indicated on the left. Levels of HCV protein expressed were normalized against endogenous actin levels (H).

carrier who was chronically infected with HCV (Lim *et al.,* 2001). We report here that this full-length HCV genome expressed its structural and nonstructural proteins when transfected into cell lines.

RANTES (regulated upon activation, normal T cell expressed and secreted) and monocyte chemoattractant protein 1 (MCP-1) are members of the CC chemokine family. MCP-1 is known to play a significant role in monocyte infiltration to sites of injury and inflammation (Leonard and Yoshmura, 1990; Schall *et al.,* 1990), while RANTES has chemotactic properties for numerous cell types, including T lymphocytes, monocytes (Schall *et al.,* 1990), and NK cells (Taub *et al.,* 1995). In addition, both chemokines have been shown to be induced by some viruses in a wide variety of cells after infection (Matikainen *et al.,* 2000; Gupta *et al.,* 2001; Haeberle *et al.,* 2001; Peterson *et al.,* 2001), including members of the flavivirus family. Induction of RANTES was observed in dengue-2 virus-infected liver cells (Lin *et al.,* 2000) and both RANTES and MCP-1 were induced during Japanese encephalitis virus infection of astrocytes (Chen *et al.,* 2000). Such a cellular response *in vivo* can serve to recruit lymphocytes and stimulate the host immune response to viral infections. Production of chemokines in

the liver is likely to play a role in HCV infection, as infiltration of lymphocytes has been observed in concomitance with chronic disease (Minutello *et al.,* 1993; Zehender *et al.,* 1997; Sansonno *et al.,* 1998; Crispe *et al.,* 2000). In this study we demonstrate that hepatitis C virus is capable of inducing MCP-1 and RANTES gene expressions in both nonhepatic and hepatic cell lines. Using cotransfection experiments with the full-length HCV cDNA, HCV-S1, we determined that the induction is initiated at the transcriptional level via activation of the transcriptional factor AP-1 in the case of MCP-1 induction, and via NF-κB and other unknown factors in RANTES. These findings have important implications in our understanding of HCV-associated liver pathogenesis.

RESULTS

Construction and characterization of expression constructs for the full-length HCV genome, HCV-S1

Nine overlapping cDNAs clones covering the entire HCV genome were obtained by RT-PCR from sera derived from a chronic HCV carrier (Lim *et al.,* 2001). These were assembled together in stepwise ligations as described under Materials and Methods. Resultant clones
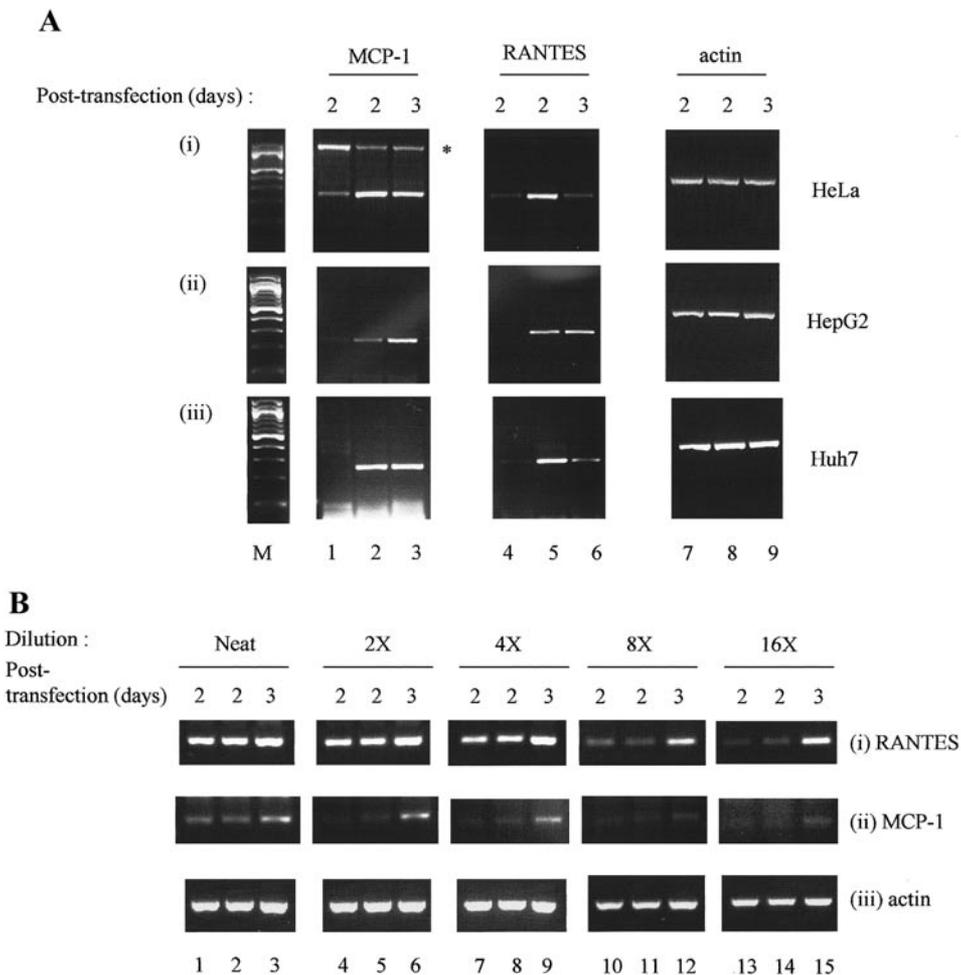
FIG. 2. (A) RT-PCR of MCP-1 (lanes 1–3) and RANTES (lanes 4–6) transcripts in (i) HeLa, (ii) Huh7, and (iii) HepG2 cells transfected with pXJ(S1) at 2 (lanes 2, 5, and 8) and 3 days (lanes 3, 6, and 9) posttransfection. As a control, cells were transfected with vector pXJ41neo for 2 days (lanes 1, 4, and 7). RT-PCR was performed on total cellular RNA extracted from cells as described under Materials and Methods (see also Table 1). Levels of endogenous actin mRNA (lanes 7–9) are shown. M indicates 100-bp DNA ladder. Asterisk indicates nonspecific bands. (B) Semiquantitative detection of (i) RANTES, and (ii) MCP-1 mRNA in HepG2 cells by RT-PCR. Cells were transfected with pXJ(S1) for 2 (lanes 2, 5, 8, 11, and 14) and 3 days (lanes 3, 6, 9, 12, and 15) or with vector pXJ41neo for 2 days (lanes 1, 4, 7, 10, and 13). Serial dilutions of cDNA samples (1:2, 1:4, 1:8, and 1:16, depicted as 2×, 4×, 8×, and 16×) were prepared and subjected to PCR as in (A). Levels of endogenous actin mRNA (iii) are shown.

comprising the region from the 5′UTR to NS2 (nt −341 to 2461) were first functionally tested by *in vitro* coupled transcription-translation to ensure that all the HCV structural proteins could be properly translated (data not shown). Clones comprising the region from the NS2-3′ UTR (nt 2428–9268) were similarly analyzed (data not shown). The full-length (FL) HCV genome was assembled from these clones to generate the expression constructs pcDNA3(S1) and pXJ41(S1). To characterize this full-length clone, we transiently transfected pXJ(S1) into 293T cells and examined the expression of HCV proteins by Western analyses. We were able to detect HCV structural (core, E1, and E2) and nonstructural (NS-3, -4B, -5A, and -5B) proteins at 2 and 4 days posttransfection (Figs. 1A–1G). Thus, the FL HCV genome could be properly transcribed and translated to yield the complete polyprotein which in turn could be processed to the individual

proteins. Transfection with the expression construct pcDNA3(S1) produced similar results, although lower HCV protein levels were observed (data not shown).

Induction of CC chemokines RANTES and MCP-1 in HCV-S1-transfected cells

Recently, a member of the flavivirus, dengue-2 virus, was shown to induce the expression of CC chemokine RANTES upon infecting liver cells (Lin *et al.,* 2000). It has also been reported by several groups that infection of some viruses leads to cellular induction of chemokines (Matikainen *et al.,* 2000; Gupta *et al.,* 2001; Haeberle *et al.,* 2001; Peterson *et al.,* 2001). This phenomenon could conceivably play an important role in determining the final outcome of the disease(s) manifested in infected individuals. We therefore set out to determine if HCV

would similarly induce the expression of RANTES or MCP-1. Using specific primers, we performed RT-PCR for these chemokines, with total cellular RNA collected from cells at 2 and 3 days posttransfection with pXJ(S1). As a control, we used RNA from cells transfected with the vector pXJ41neo. We found strong inductions of both RANTES and MCP-1 transcripts in the epithelial cell line, HeLa, as well as in the hepatoma cell lines, Huh7 and HepG2 (Fig. 2A). In addition, we observed that induction of RANTES mRNA appeared to be more tightly regulated as its levels began to decline by day 3 posttransfection in two of the three cell lines (HeLa and Huh7). In contrast, induction of MCP-1 transcripts appeared to be either sustained (in HeLa and Huh7) or increased (in HepG2) at 3 days after transfection (Fig. 2A). We next performed a semiquantitative PCR analyses for RANTES and MCP-1 expression in HepG2 cells using serial dilutions of the cDNA samples. We observed that HCV-mediated induction of both MCP-1 and RANTES was associated with an at least 16-fold increase over basal transcripts levels 3 days after expression of HCV proteins in HepG2 cells (Fig. 2B). Furthermore, we detected increased levels of RANTES and MCP-1 proteins in pXJ(S1)-transfected cells by FACscan analysis using intracellular staining with specific antibodies to these chemokines (Fig. 3). Three days after transfection with the HCV genome, intracellular levels of RANTES protein in HeLa cells were higher than those of cells transfected with the vector pXJ41neo (Figs. 3A and 3B). In addition, intracellular MCP-1 levels were also increased (Figs. 3C and 3D). A similar trend was also observed in HCV-transfected Huh7 (Figs. 3E–3H) and HepG2 cells (Figs. 3I–3L). Expression of FL HCV therefore induces the expression of the chemokines in both hepatic and nonhepatic cell lines.

HCV genome activates promoters of RANTES and MCP-1

To further investigate the activation of MCP-1 and RANTES by FL HCV at the transcriptional level, we carried out transient cotransfection experiments with pXJ(S1) and 5′ deletion promoter constructs of MCP-1 (Lim and Garzino-Demo, 2000) and RANTES (Nelson *et al.,* 1993, 1996). We found that FL HCV significantly stimulated luciferase activities of deletion promoter constructs of both these genes in HeLa and Huh7 cells (Fig. 4). In the case of MCP-1, the construct, phMCP213, bearing a 213 base pair (bp) of the MCP-1 promoter was induced by 3.6-fold over basal levels in HeLa cells, while the activity of phMCP128, containing a 128-bp fragment, was increased by 2.4-fold at 48 h posttransfection (Fig. 4A). When the experiments were repeated in Huh7 cells, the activities of these constructs were found to be augmented by 2.9- and 2-fold, respectively, above basal levels (Fig. 4B). These results suggest that the region comprising 128 bp upstream from the translational start
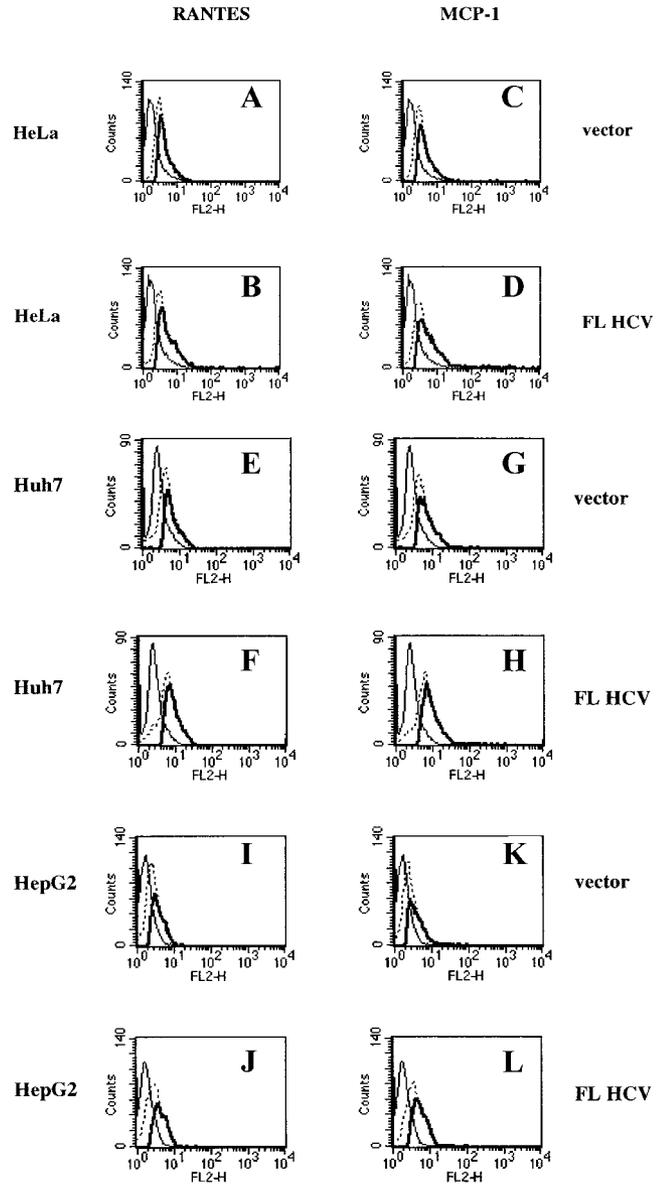
FIG. 3. FACscan analyses of HeLa (A–D), Huh7 (E–H), and HepG2 (I–L) cells transfected with vector, pXJ41neo (A, C, E, G, I, and K), or full-length (FL) HCV construct, pXJ(S1) (B, D, F, H, J, and L) at 3 days posttransfection. Intracellular staining was carried out with PE-conjugated antibodies specific for MCP-1 (C, D, G, H, K, and L) or RANTES (A, B, E, F, I, and J) as described under Materials and Methods. Solid line (—) denotes unstained cells; dotted line (- -) denotes cells stained with specific antibodies, and bold solid line (▬) denotes the final fluorescence after subtracting the first (background) from the second.

site of MCP-1 contained sufficient binding elements to enable the gene to be optimally activated by HCV, although additional binding elements within the region from nt 128 to nt 213 could also participate to augment gene activation. Thus it appears that the AP-1 and NF-κB sites located at positions −150 and −137, respectively, are less important in HCV-mediated MCP-1 induction than downstream binding motifs such as the SP-1 (at −115), NF-1 (at −70), and the second AP-1 site (at −122).
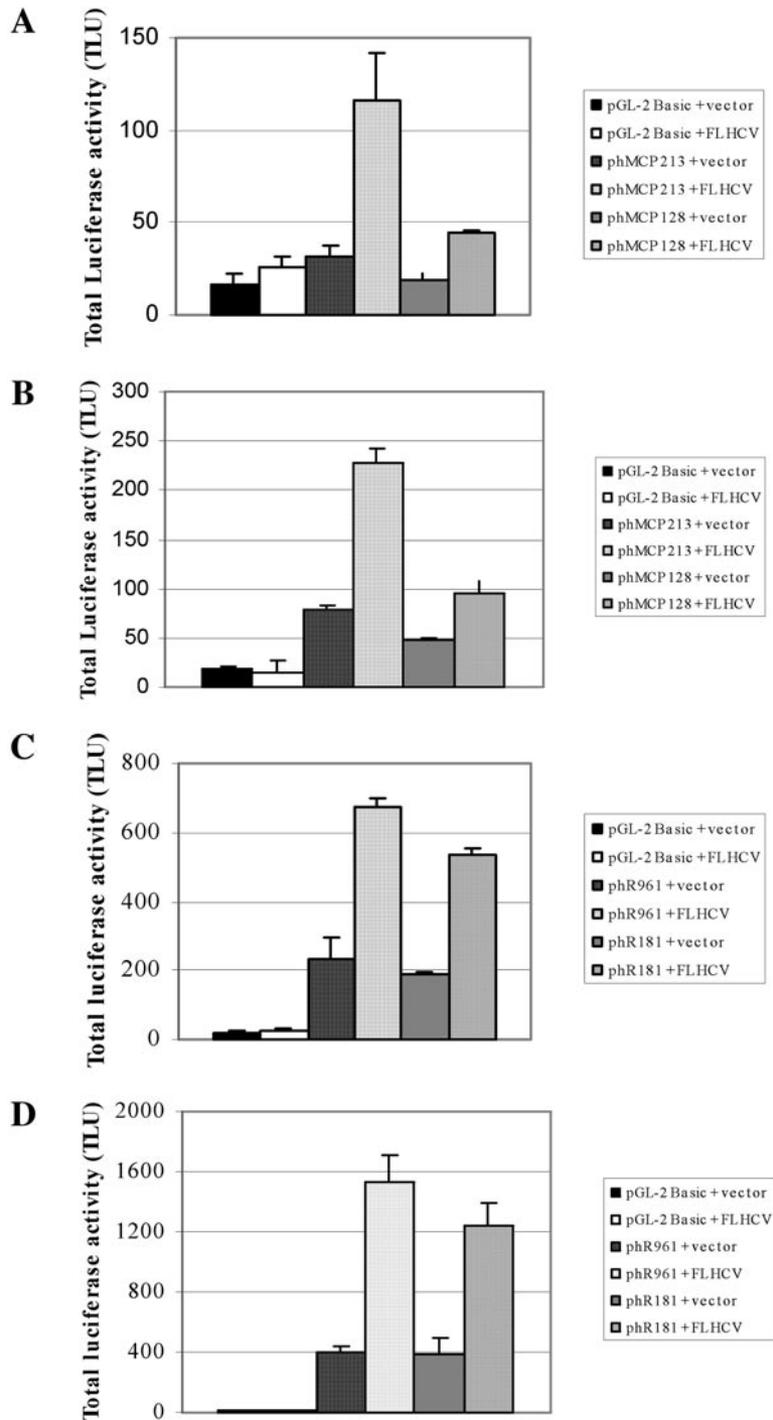
FIG. 4. Deletion analysis of the HCV-mediated up-regulation of 5′ flanking regions of MCP-1 and RANTES. Luciferase assays were performed with extracts of HeLa cells (A and C) and Huh7 (B and D) cells transfected with different 5′ deletion constructs for MCP-1 (A and B) or RANTES (C and D), at 48 h posttransfection. Results are expressed as the absolute luciferase activity in each cell extract and were normalized according to units of renilla luciferase activity from cotransfection with a pTK-renilla luciferase construct and total protein content. Data shown are the means (±SD) of three independent transfection experiments.

We next examined the effect of HCV on the activities of deletion constructs for the RANTES promoter. The construct, phR961, which bears a 961 bp of its promoter sequence, was induced by 2.9-fold over basal levels in HeLa cells, while phR181, which contains a 181-nt sequence immediately upstream of the promoter, was increased by 2.8-fold (Fig. 4C). In Huh7 cells, their activities were also comparable; the former was stimulated by

SOO ET AL.
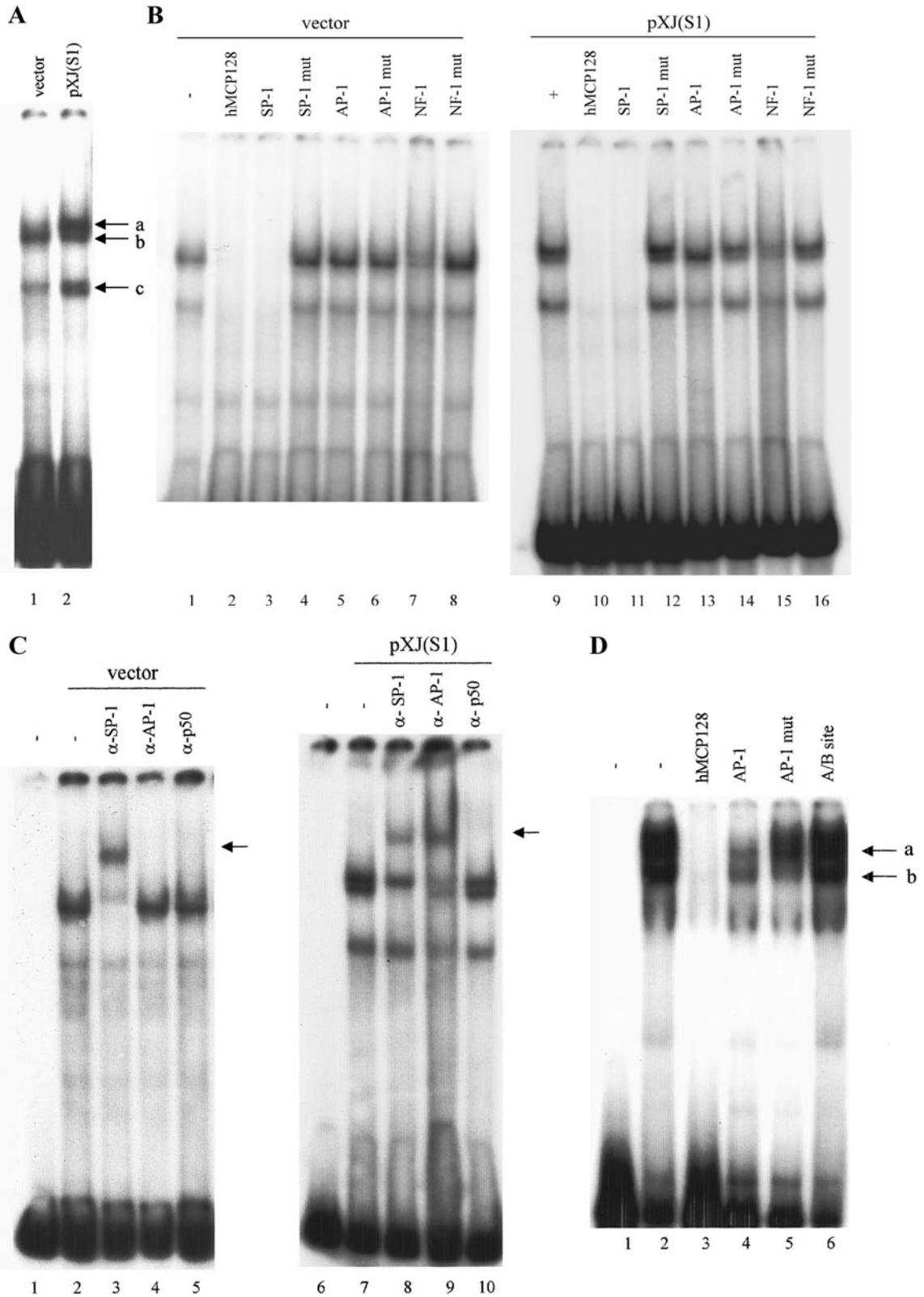
FIG. 5. HCV enhanced binding of transcriptional factors to MCP-1 promoter region. (A) A radiolabeled DNA fragment containing from −128 to +6 bp from the hMCP-1 5′ flanking region was incubated with nuclear extracts from vector-transfected (lane 1) or pXJ(S1)-transfected (lane 2) Huh7 cells. Arrows indicate specific DNA–protein complexes. (B) Lanes 1–8 represent EMSAs with nuclear extracts from vector-transfected Huh7 cells, while lanes 9–16 represent EMSAs with nuclear extracts from pXJ(S1)-HCV-transfected Huh7 cells. Competition assays were performed with 100-fold molar excess of unlabeled DNA fragments corresponding to the −128 to +6 hMCP-1 5′ flanking region (lanes 2 and 10) or 100-fold molar excess of

3.8-fold above control cells and the latter was stimulated by 3.2-fold above control cells (Fig. 4D). Thus, it appears that the minimal construct containing 181 bp of the RANTES promoter region was sufficient for maximal gene activation by HCV. Interestingly, this suggests that transcriptional binding elements upstream of this minimal region, such as the three AP-1 sites at −402, −420, and −429 (Nelson et al., 1993), do not participate in HCV-mediated induction of RANTES.

HCV genome induces AP-1 binding activities at minimal hMCP-1 promoter region, hMCP128

The 128-nt upstream region of the MCP-1 promoter contains putative cis-acting elements for AP-1 (−122), SP-1 (−115), NF-1 (−70), and CAAT (−33) (Shyy et al., 1993; Li and Kolattukudy, 1994; Lim and Garzino-Demo, 2000). To explore the roles of these various cis-acting elements in the HCV-mediated up-regulation of the MCP-1 gene, we conducted electrophoretic mobility shift assays (EMSAs) with this region of the gene as probe. Nuclear extracts prepared from vector-transfected Huh7 cells produced two distinct DNA–protein complexes when shifted with a radiolabeled DNA fragment corresponding to region −128 to +6 of the hMCP promoter (hMCP128; Fig. 5A, lane 1, bands b and c). Binding of both complexes was completely competed out by excess unlabeled probe, as well as by excess unlabeled oligonucleotides with a consensus SP1-binding motif (Fig. 5B, lanes 2 and 3). In addition, they were partially competed out by excess unlabeled oligonucleotides containing the NF-1 binding sequences (Fig. 5B, lane 7). In contrast, excess unlabeled oligonucleotides bearing consensus AP1-binding motifs, as well as oligonucleotides with mutated SP-1, AP-1 and NF-1 sites, failed to abolish the DNA–protein complexes (Fig. 5B, lanes 4, 6, and 8).

Interestingly, when we repeated the EMSAs with nuclear extracts prepared from FL-HCV-transfected Huh7 cells, we observed the formation of a new complex of higher mobility (Fig. 5A, lane 2, band a), in addition to the two DNA–protein complexes (bands b and c) previously observed in the untransfected cells. Binding of complexes a, b, and c were disrupted by excess unlabeled probe, and also by excess cold SP-1 (Fig. 5B, lanes 10 and 11) and partially by NF-1 oligonucleotides (Fig. 5B, lane 15). Notably, the binding of complex a was abolished by excess cold AP-1 oligonucleotides (Fig. 5B, lane 13). Similar to gel-shift assays performed with vector-transfected cells, oligonucleotides with mutated SP-1, AP-1, and NF-1 sites failed to abolish any interaction between hMCP128 and the nuclear complexes (Fig. 5B, lanes 12, 14, and 16). Hence the results from the EMSAs with hMCP128 provide strong evidence for the HCV-mediated induction of AP-1 binding activities on the MCP-1 promoter.

To determine the specificity of interaction between the DNA-binding complexes and hMCP128, we conducted supershift assays with antibodies against SP-1, AP-1, and p50. With extracts prepared from vector-transfected cells, complex b was specifically supershifted by SP-1 antibodies (Fig. 5C, lane 3, supershift is denoted by arrow) but not by AP-1 or p50 antibodies (Fig. 5C, lanes 4 and 5). With extracts prepared from HCV-transfected cells, complex b was specifically supershifted by SP-1 antibodies (Fig. 5C, lane 6, supershift is denoted by arrow), while all three complexes a–c were supershifted by AP-1 antibodies (Fig. 5C, lane 7, supershift is denoted by arrow). Anti-p50 antibodies failed to induce any supershift in the complexes (Fig. 5C, lane 8). These results confirm that while SP-1 was involved in the constitutive regulation of MCP-1, HCV induced the binding of AP-1, which cooperated with SP-1 in the HCV-mediated up-regulation of MCP-1.

To further investigate if AP-1 is capable of binding to the AP-1 site in the minimal MCP-1 promoter sequence, we conducted gel shifts using recombinant AP-1 (rAP-1) with hMCP128. We observed the formation of two DNA-binding complexes, band a and b, following the incubation of rAP-1 with hMCP128 (Fig. 5D). These two complexes were completely inhibited by addition of excess cold hMCP128 (Fig. 5D, lane 2) or double-stranded AP-1 oligonucleotides (Fig. 5D, lane 4). In contrast, they were poorly inhibited by competition with excess cold mutated AP-1 oligonucleotides (Fig. 5D, lane 5) and cold oligonucleotides corresponding to the A/B site in hRAN181 (Fig. 5D, lane 6).

HCV genome enhances binding activities to A/B site on the minimal hRANTES promoter region, hRAN181

In the 181-nt upstream region of the RANTES promoter, putative binding domains for NF-κB (−102), C/EBP (−119), AP-3 (−119), CCAAT (−142), and NF IL-6 (−164) have been identified (Nelson et al., 1993). We performed similar experiments using a radiolabeled DNA fragment corresponding to this region of the RANTES promoter

unlabeled specific oligonucleotides (lanes 3–8 and 11–16) as indicated. (C) EMSAs supershifts performed with nuclear extracts from vector-transfected Huh7 cells (lanes 2–5), or pXJ(S1)-HCV-transfected Huh7 cells (lanes 6–10), using specific antibodies against SP-1 (lanes 3 and 8), AP-1 (lanes 4 and 9), and p50 (lanes 5 and 10). Lane 1 consists of free probe. Arrow denotes supershifted complex. (D) EMSAs performed with recombinant AP-1 proteins and the −128 to +6 hMCP-1 5′ flanking region (lanes 2–6). Competition assays were performed with 100-fold molar excess of unlabeled DNA fragments corresponding to the −128 to +6 hMCP-1 5′ flanking region (lane 3), the A/B site in the minimal RANTES promoter sequence (lane 6) or 100-fold molar excess of unlabeled specific AP-1 (lane 4) and mutated AP-1 oligonucleotides (lane 5). Lane 1 consists of free probe. Arrows indicate specific DNA–protein complexes.

(hRAN181; Fig. 6). Nuclear extracts prepared from vector-transfected Huh7 cells produced two DNA–protein complexes of very similar mobility (Fig. 6A, lane 1, bands a and b), while transfection with FL HCV in Huh7 cells led to an overall increase in DNA-binding activities of both complexes (Fig. 6A, lane 2). Binding of these complexes was completely competed out by excess unlabeled probe (Fig. 6B, lanes 2 and 9). Interestingly, binding of complexes a and b in untransfected cells was successfully disrupted by excess unlabeled oligonucleotides with the A/B site (nt -131 to -103) (Fig. 6B, lane 3), which contains a sequence homologous to the κB-binding motif. Competition was thus carried out with oligonucleotides bearing consensus NF-κB sites. These too competed out both the DNA–complex formations (Fig. 6B, lane 4), indicating that κB-binding factors were involved in constitutive RANTES expression.

Similarly, in the HCV-transfected cells, unlabeled A/B site and NF-κB oligonucleotides inhibited formations of the complexes (Fig. 6B, lanes 10 and 11). The effect of competition with A/B site oligonucleotides was more pronounced than with NF-κB oligonucleotides, suggesting that FL HCV induced the binding of other factors besides members of the NF-κB/Rel family to this site. On the other hand, excess unlabeled NF-IL6 oligonucleotides failed to disrupt any DNA–protein complex formation in extracts prepared from both untransfected and transfected cells (Fig. 6B, lanes 6 and 13), implying that NF-IL6 does not play a significant role in HCV-mediated induction of RANTES gene expression. Oligonucleotides with mutated NF-κB and NF-IL6 sites also failed to compete out binding of DNA–protein complexes (Fig. 6B, lanes 5, 7, 12, and 14). Hence, the results from these EMSA experiments suggest that HCV-induced binding activities to the A/B site on hRAN181 are important in mediating the up-regulation of the RANTES gene. To ascertain this, we performed further gel-shift assays, using the A/B sequence as a probe. Indeed, transfection of Huh7 cells with the FL HCV genome led to a marked increase in A/B binding activities, compared to control vector-transfected cells (Fig. 7A, compare lanes 1 and 2). Three DNA–protein complexes were observed (bands a, b, and c) of which the complex of lowest mobility (band a) was most strongly induced by HCV (Fig. 7A). The DNA–protein complexes were specifically disrupted by excess unlabeled A/B oligonucleotides (Fig. 7B, lanes 2 and 6). Similar to our previous observation on the -181-bp region, A/B binding activities were only partially disrupted by excess unlabeled NF-κB oligonucleotides (Fig. 7B, lanes 3 and 7), confirming that HCV induced other factors that bind to this site which may play a role in enhancing RANTES gene expression. Interestingly, mutated NF-κB oligonucleotides also marginally competed out binding at the A/B site (Fig. 7B, lanes 4 and 8). The reason for this is unknown, but, it is possible that

other A/B binding proteins could still interact with the GC-rich region within this sequence.

To confirm that NF-κB is involved in binding to hRAN181 and A/B sequences, we further carried out supershift assays with p50 and p65 antibodies. Both antibodies supershifted DNA complexes a and b in nuclear extracts prepared from vector- and HCV-transfected cells in gel shifts performed with hRAN181 (Fig. 6C, lanes 3, 4, 7, and 8; supershifts are denoted by arrow) as probe. When the A/B sequence was used as a probe, the antibodies mainly supershifted DNA complex a (Fig. 7C, lanes 3, 4, 7, and 8; supershifts are denoted by arrow). The control antibodies against AP-1 failed to induce any supershift in extracts prepared from vector- (Figs. 6C and 7C, lane 5) or HCV- (Figs. 6C and 7C, lane 9) transfected cells. Furthermore, when recombinant p50 proteins were incubated with the A/B sequence, two complexes, consisting of a major band a and a minor band b, were observed (Fig. 7D, lane 2). Formation of both bands was completely abolished by competition with excess cold oligonucleotides corresponding to the A/B sequence (Fig. 7D, lane 3) and cold NF-κB double-stranded oligonucleotides (Fig. 7D, lane 4). On the other hand, these complexes were not competed out by excess cold mutated NF-κB oligonucleotides (Fig. 7D, lane 5) or cold hMCP128 element (Fig. 7D, lane 6).

Full-length HCV up-regulates AP-1 and NF-κB activities

Based on our transfection experiments and EMSAs, AP-1 appears to play an important role in FL HCV-mediated induction of MCP-1, and NF-κB is involved in the induction of RANTES. To confirm that the FL HCV genome which we have constructed is indeed able to induce these two transcriptional factors, we carried out additional cotransfection experiments with pXJ(S1) and luciferase reporter constructs containing consensus binding elements for AP-1 or NF-κB. Two days posttransfection, AP-1-driven luciferase activities in HeLa cells transfected with FL HCV were 3.2-fold above those of cells transfected with vector alone (Fig. 8A). This level of induction was comparable to that for NF-κB-driven luciferase activities which were increased by 2.9-fold over the same period in the same cell line (Fig. 8B). Similarly, both AP-1 and NF-κB induced activities were enhanced by 3.3- and 3.4-fold, respectively, in FL HCV-transfected Huh7 (Figs. 8C and 8D). These results confirmed the ability of the FL HCV to induce both *trans*-activating factors and suggest that these proteins have different *trans*-activating effects on different CC chemokine genes. We hypothesize that while AP-1 binding proteins are involved in FL HCV-mediated induction of MCP-1, they are not important for HCV-mediated induction of RANTES. Conversely, NF-κB binding activities do not play a significant role in the FL HCV-mediated up-regu-
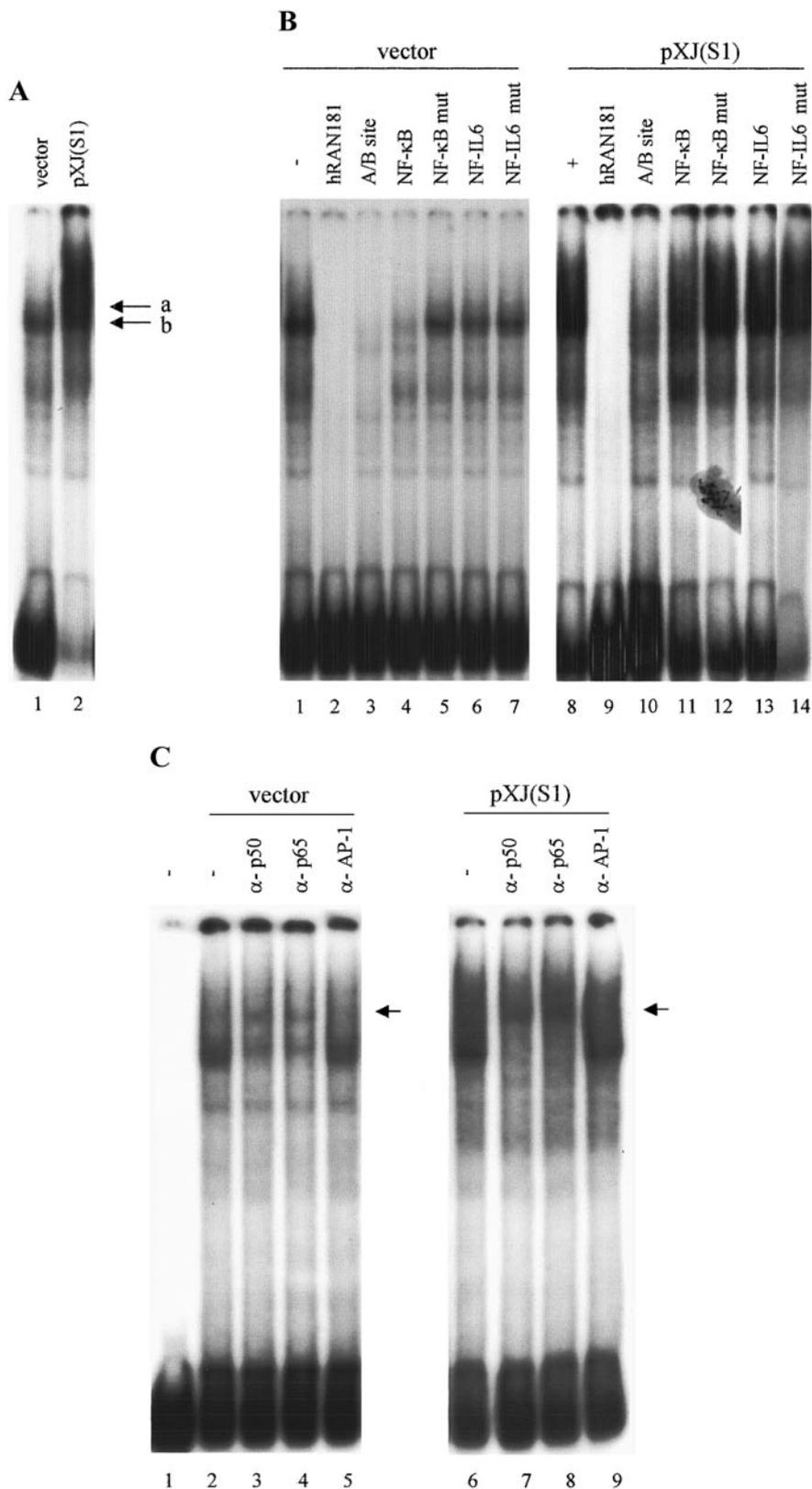
FIG. 6. HCV enhanced binding of transcriptional factors to RANTES promoter region. (A) A radiolabeled DNA fragment containing from -181 to $+6$ bp from the hRANTES 5′ flanking region was incubated with nuclear extracts from vector-transfected (lane 1) or pXJ(S1)-transfected (lane 2) Huh7 cells. Arrows indicate specific DNA–protein complexes. (B) Lanes 1–7 represent EMSAs with nuclear extracts from vector-transfected Huh7 cells, while lanes 8–14 represent EMSAs with nuclear extracts from pXJ(S1)-transfected Huh7 cells. Competition assays were performed with 100-fold molar excess of unlabeled DNA fragments corresponding to the -181 to $+6$ hRANTES 5′ flanking region (lanes 2 and 9) or 100-fold molar excess of unlabeled specific oligonucleotides (lanes 3–7 and 10–14) as indicated. (C) EMSAs supershift assays performed with nuclear extracts from vector-transfected Huh7 cells (lanes 2–5), or pXJ(S1)-transfected Huh7 cells (lanes 6–9), using specific antibodies against p50 (lanes 3 and 7), p65 (lanes 4 and 8), and AP-1 (lane 5 and 9). Lane 1 consists of free probe. Arrow denotes supershifted complex.
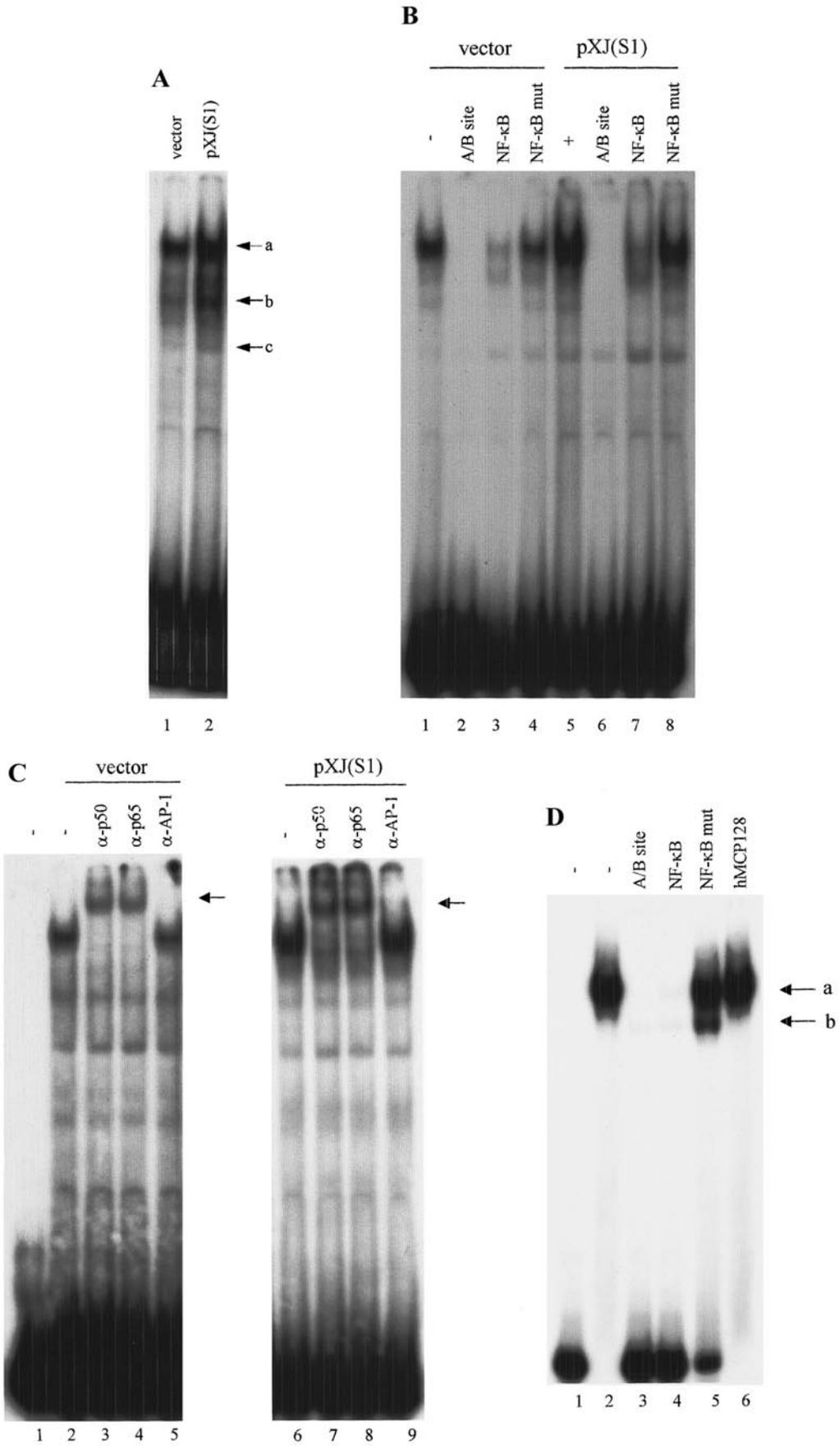
lation of MCP-1 expression, but they cooperate with unknown factors during HCV-mediated up-regulation of RANTES expression.

HCV proteins differentially activate NF-κB and RANTES promoter in HeLa and Huh7 cells

Results from the gel-shift and luciferase reporter assays indicated that binding of NF-κB to the RANTES promoter was induced upon expression of HCV proteins. To further investigate the particular HCV protein(s) that was responsible for the induction of NF-κB, we carried out further transfection experiments using expression constructs for various HCV proteins. The induction levels are summarized in Table 1. In HeLa cells, both core and NS5A up-regulated the activity of the NF-κB luciferase reporter construct (Fig. 9A, Table 1). Transfection of core markedly increased the NF-κB activities by 11.4-fold over the basal levels (Fig. 9A, Table 1). Transfection with either NS5A or the full-length HCV construct led to a more moderate increase of 2.6-fold over basal levels (Fig. 9A, Table 1). A construct bearing all the nonstructural HCV proteins (NSP) gave a comparable increase as NS5A and the full-length genome (2.9-fold above basal levels), suggesting that other nonstructural proteins do not enhance NF-κB activities (Fig. 9A, Table 1). Also a construct bearing all the structural proteins (SP) failed to induce any NF-κB activities (Fig. 9A, Table 1), suggesting that the structural proteins E1 and E2 did not activate NF-κB and may instead inhibit the activity of core.

We then examined at the effects of HCV proteins on the minimal RANTES promoter construct, phR181 in HeLa cells. We observed that core and NS5A induced RANTES promoter activities by 5.2- and 2.8-fold, respectively, over basal levels (Fig. 9B, Table 1). This was comparable to the levels induced by the NSP and the full-length HCV constructs, which increased its activities by 3.9- and 5.6-fold, respectively (Fig. 9B, Table 1). The SP construct produced a smaller increase of twofold (Fig. 9B, Table 1), suggesting again that other structural proteins may inhibit core activity on the RANTES promoter. Thus, in HeLa cells activation of NF-κB and RANTES promoter activities appear to be mediated mainly by core and NS5A.

We then repeated these experiments with the reporter constructs for NF-κB and the RANTES promoter in the human hepatoma cell line, Huh7. Similar to the observation in HeLa cells, NS5A, NSP, and full-length HCV genome increased the activity of the NF-κB luciferase reporter construct to comparable levels of 2.4-, 3.2-, and 3.1-fold, respectively (Fig. 9C, Table 1). Transfection of SP construct again failed to induce NF-κB activities (Fig. 9C, Table 1). Rather surprisingly, in contrast to the observation in HeLa cells, core strongly reduced NF-κB activities in Huh7 cells. The levels were decreased by 58% compared to the basal levels (Fig. 9C, Table 1). We then proceeded to study the effect of these various HCV proteins on the RANTES promoter construct, phR181, in Huh7 cells. Similar to our findings on the NF-κB construct, core also significantly suppressed RANTES promoter activity by 70% (Fig. 9D, Table 1), while NS5A, NSP, and full-length HCV genome constructs increased its activity by 2.7-, 6.8-, and 6.8-fold, respectively (Fig. 9D, Table 1). Similar to in HeLa cells, the SP construct induced RANTES promoter activity by twofold (Fig. 9D, Table 1). Therefore, in Huh7 cells induction of NF-κB and RANTES promoter activities appears not to be mediated by core, but by NS5A. In addition, in Huh7 cells, other nonstructural protein(s) may activate RANTES via an NF-κB independent mechanism. Finally, in Huh7 cells, HCV structure proteins E1 and E2 could weakly activate the RANTES promoter by a mechanism that also may not involve NF-κB.

## HCV proteins differentially activate AP-1 and MCP-1 promoter in HeLa and Huh7 cells

Results from the gel-shift and reporter transfection assays indicated that binding of AP-1 to the MCP-1 promoter was induced upon expression of HCV proteins. To ascertain if HCV core, NS5A, and/or other HCV proteins induced the expression of AP-1, we again carried transfection experiments using expression constructs for these proteins. In HeLa cells, core up-regulated the activity of the AP-1 reporter construct by threefold above basal levels (Fig. 10A, Table 1). As was observed previously for the NF-κB construct, the SP construct failed to induce any AP-1 activities (Fig. 10A, Table 1). This also

FIG. 7. HCV enhanced binding of transcriptional factors to A/B site in the RANTES promoter region. (A) A radiolabeled double-stranded oligonucleotide containing A/B site of the hRANTES 5′ flanking region was incubated with nuclear extracts from vector- (lane 1) or pXJ(S1)-transfected (lane 2) Huh7 cells. Arrows indicate specific DNA–protein complexes. (B) Lanes 1–4 represent EMSAs with nuclear extracts from vector-transfected Huh7 cells, while lanes 5–8 represent EMSAs with nuclear extracts from pXJ(S1)-transfected Huh7 cells. Competition assays were performed with 100-fold molar excess of double-stranded unlabeled oligonucleotides corresponding to A/B site (lanes 2 and 6) or 100-fold molar excess of unlabeled specific oligonucleotides (lanes 3–4 and 7–8) as indicated. (C) EMSAs supershift assays performed with nuclear extracts from vector-transfected Huh7 cells (lanes 2–5), or pXJ(S1)-transfected Huh7 cells (lanes 6–9), using specific antibodies against p50 (lanes 3 and 7), p65 (lanes 4 and 8), and AP-1 (lane 5 and 9). Lane 1 consists of free probe. Arrow denotes supershifted complex. (D) EMSAs performed with recombinant p50 proteins and radiolabeled double-stranded oligonucleotides containing A/B site of the hRANTES 5′ flanking region (lanes 2–6). Competition assays were performed with 100-fold molar excess of unlabeled oligonucleotides corresponding to the A/B site in hRANTES promoter (lane 3), NF-κB (lane 4), and mutated NF-κB (lane 5) and excess unlabeled DNA fragments corresponding to the −128 to +6 of the 5′ flanking region of hMCP128. Lane 1 consists of free probe. Arrows indicate specific DNA–protein complexes.
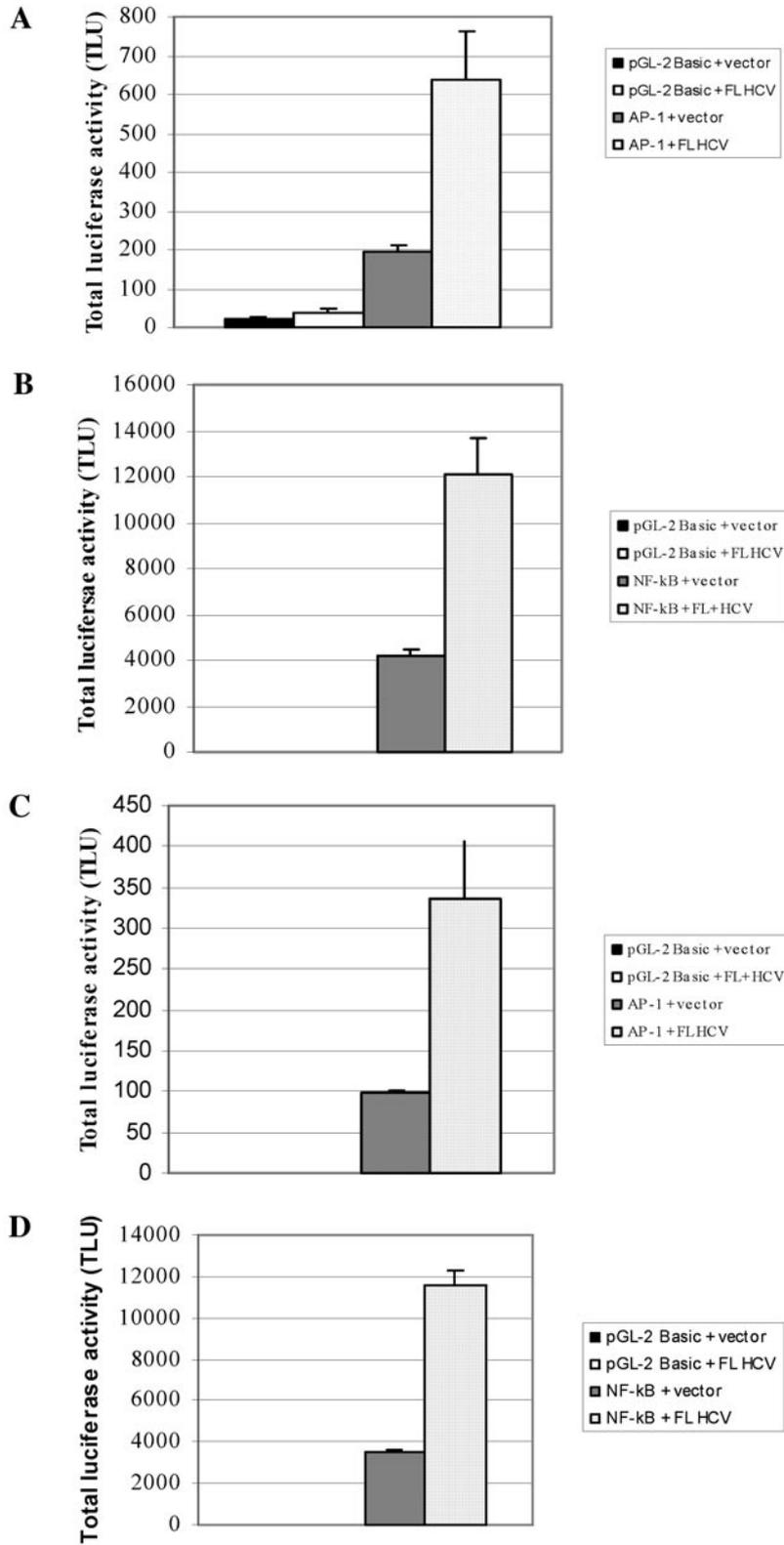
FIG. 8. HCV-mediated up-regulation AP-1 and NF-κB activities. Luciferase assays were performed with extracts of HeLa cells (A and B) and Huh7 (C and D) cells cotransfected with reporter constructs for AP-1 (A and C) or NF-κB (B and D) and the full-length (FL) HCV expression construct, pXJ(S1), at 48 h posttransfection. Results are expressed as the absolute luciferase activity in each cell extract and were normalized according to units of renilla luciferase activity from cotransfection with a pTK-renilla luciferase construct and total protein content. Data shown are the means (±SD) of three independent transfection experiments.
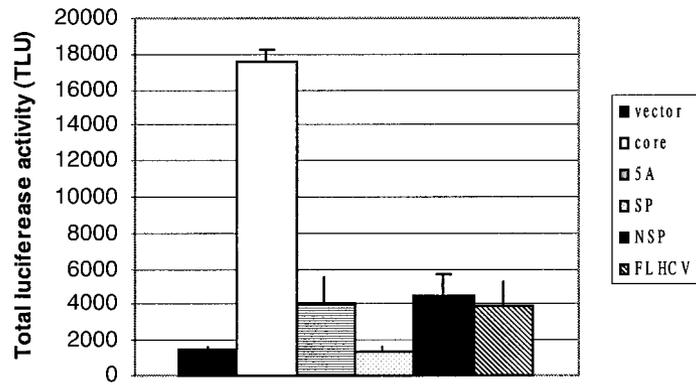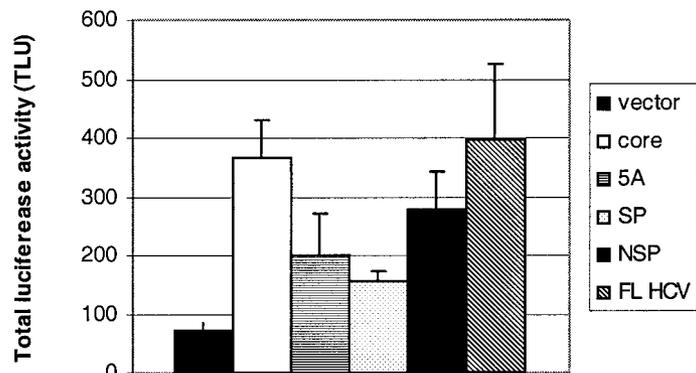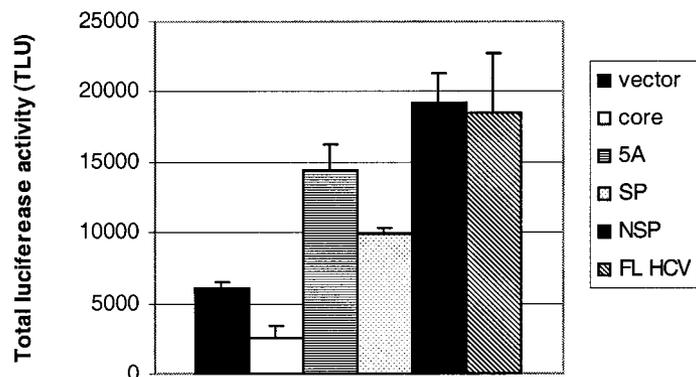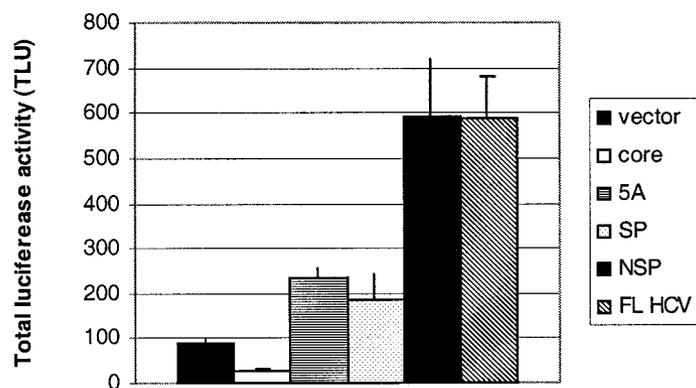
FIG. 9. Effect of various HCV proteins on the activities of the NF-κB and minimal RANTES promoter reporter constructs. Luciferase assays were performed with extracts of HeLa cells (A and B) and Huh7 (C and D) cells cotransfected with reporter constructs for NF-κB (A and C) or RANTES promoter, phR181 (B and D), and the various expression constructs for HCV proteins, at 35 h posttransfection. Transfection was performed with the empty vector, pXJ41neo, to determine basal luciferase levels. SP, NSP, and FL HCV denote expression constructs for HCV structural proteins, nonstructural proteins, and full-length HCV genome, respectively. Results are expressed as the absolute luciferase activity in each cell extract and were normalized according to total protein content. Data shown are the means (±SD) of three to five independent transfection experiments.

A HeLa + AP-1
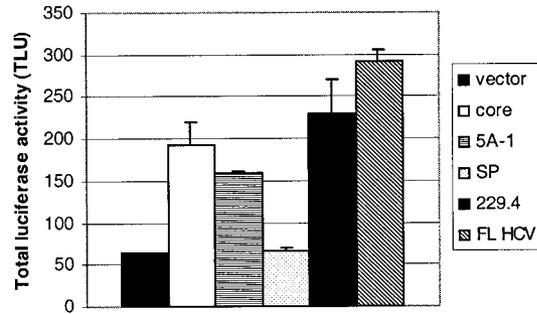
B HeLa + phMCP128
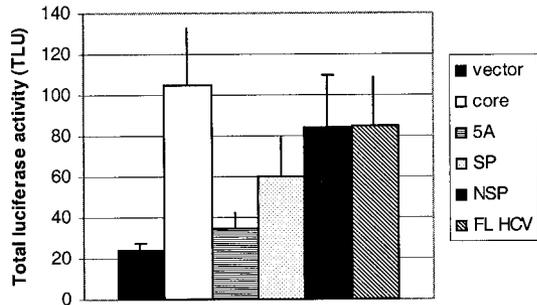
C Huh7 + AP-1
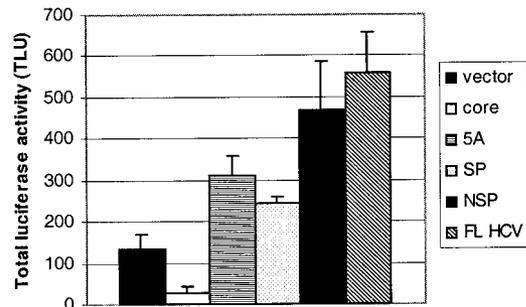
D Huh7 + phMCP128
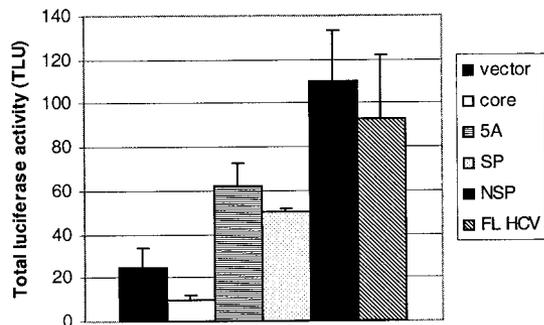
FIG. 10. Effect of various HCV proteins on the activities of AP-1 and minimal MCP-1 promoter reporter constructs. Luciferase assays were performed with extracts of HeLa cells (A and B) and Huh7 (C and D) cells cotransfected with reporter constructs for AP-1 (A and C) or MCP-1 promoter, phMCP128 (B and D), and the various expression constructs for HCV proteins, at 35 h posttransfection. Transfection was performed with the empty vector, pXJ41neo, to determine basal luciferase levels. SP, NSP, and FL HCV denote expression constructs for HCV structural proteins, nonstructural proteins, and full-length HCV genome, respectively. Results are expressed as the absolute luciferase activity in each cell extract and were normalized according to total protein content. Data shown are the means (±SD) of three to five independent transfection experiments.

implies that the structural proteins E1 and E2 did not activate AP-1 and could suppress the activity of core. The NSP and NS5A constructs both induced AP-1 activities by 2.5- and 3.6-fold, respectively, over basal levels, while the full-length genome activated AP-1 by 4.6-fold (Fig. 10A, Table 1). Thus, similar to the observation for NF-κB

activation, it appears that in HeLa cells, AP-1 activities are mediated mainly by both core and NS5A proteins, while structural proteins could inhibit core-mediated AP-1 activities.

We next sought to determine the effects of HCV proteins on the MCP-1 promoter in HeLa cells, using the

minimal construct, phMCP128. Akin to the results obtained with the RANTES reporter construct, HCV core increased MCP-1 promoter activity by 4.3-fold over basal levels (Fig. 10B, Table 1), while the SP construct increased its activity to a lesser extent (2.5-fold; Fig. 10B, Table 1). The constructs for NS5A, NSP, and full-length HCV genome increased the activity of the AP-1 luciferase reporter construct to comparable levels of 3.0-, 3.5-, and 3.5-fold, respectively. Thus it appears that in HeLa cells, core and NS5A are mainly responsible for activating MCP-1 gene and other nonstructural proteins do not activate MCP-1.

The transfection experiments with the reporter constructs for AP-1 and the MCP-1 promoter were then repeated in the human hepatoma cell line, Huh7. As was observed with the NF-κB and RANTES minimal promoter constructs, core significantly decreased AP-1 activities in Huh7 cells. Its binding activities were reduced by 80% over the basal levels (Fig. 10C, Table 1). The SP construct likewise did not significantly induce AP-1 promoter activity (Fig. 10C, Table 1). Rather NS5A, NSP, and full-length HCV genome constructs increased the activity of the AP-1 reporter construct to similar levels, by 2.3-, 3.5-, and 4.2-fold, respectively, over basal levels. Transfection experiments with the minimal MCP-1 promoter construct, phMCP128, in Huh7 cells revealed that core likewise suppressed its activity. In the presence of core, the luciferase activities were 62% less than the basal levels (Fig. 10D, Table 1). Similar to the results obtained in HeLa cells, the SP construct weakly induced MCP-1 promoter activity by 2.4-fold (Fig. 10D, Table 1). On the other hand, NS5A, NSP, and full-length HCV genome constructs increased its activity by 2.5-, 4.5-, and 3.8-fold, respectively. Thus, in summary, in Huh7 cells, induction of AP-1 and MCP-1 promoter activities parallels the profile observed with NF-κB and RANTES promoter. Promoter induction in this context is not mediated by core, but by NS5A. In addition, in Huh7 cells, E1 and E2 may also activate MCP-1 via an AP-1 independent mechanism.

Expression of HCV core and NS5A proteins following transfection in HeLa and Huh7 cells

Our luciferase reporter studies indicated that HCV core has different effects on gene regulation in the two cell lines, HeLa and Huh7. HCV core has been shown to exist in several different isoforms, with sizes of 21, 19 (Hussy et al., 1996; Lo et al., 1995), or 16 kDa (Lo et al., 1995). Moreover, the p16 isoform has been reported to be localized to the nucleus, while the larger forms are found in the cytoplasm (Watashi et al., 2001; Lo et al., 1995; Suzuki et al., 1995). Retention of core in the cytoplasm is also believed to be necessary for its ability to activate NF-κB (Watashi et al., 2001). To investigate if the difference in core-mediated NF-κB and AP-1 activities observed in HeLa and Huh7 cells were due to different

processing of the core protein, we first performed Western analyses on these cell lines transfected with expression constructs for either core, SP, or full-length HCV. To this end, we used lysates obtained from our previous transfection experiments with the phR181 construct. Core activated phR181 only in HeLa cells and not in Huh7 cells (Fig. 9). Two bands with molecular weights of about 17 and 16 kDa were detected in both cell lines transfected with core, SP, or full-length HCV genome, using anticore-specific antibodies (Figs. 11A and 11B, lanes 2–4). No signal was detected in cell lysates from vector-transfected cells, used as a control (Figs. 11A and 11B, lane 1). Thus the difference in core-mediated gene regulation is not due to different processing of the core in HeLa and Huh7 cells. As a control, we also examined the expression of NS5A in these two cell lines. A major band of about 58 kDa was observed in lysates of cells transfected with constructs expressing NS5A, NSP, and full-length HCV genome (Figs. 11C and 11D). We next examined the localization of the core protein in these two cell lines. HeLa and Huh7 cells were transfected with expression constructs for core, SP, and full-length HCV genome and indirect immunofluorescence was performed using anticore antibodies. In all cases, strong staining was observed in the cytoplasm (Figs. 12A and 12B). Control cells transfected with an empty vector alone failed to give any staining (Fig. 12). Nevertheless, there was a difference in the staining pattern observed between HeLa and Huh7 cells. In the former, the staining was relatively even and diffused throughout the cytoplasm (Fig. 12A), while in the latter, strong staining concentrated at the perinuclear regions was observed (Fig. 12B), suggesting that core protein was mainly localized in the endoplasmic reticulum.

HCV up-regulates the expression of AP-1 mRNA

We observed that HCV up-regulated AP-1 protein binding activities (Fig. 13). We therefore sought to determine if HCV could induce the expression of members of the AP-1 family at the transcriptional level. To do this, we carried out RT-PCR using primers specific for c-jun with total cellular RNA from cells transfected with pXJ(S1). We used RNA obtained from cells transfected with the vector pXJ41neo as our control. We observed that c-jun transcripts were induced in HeLa, Huh7, and HepG2 2 days posttransfection with FL HCV (Fig. 13A). Interestingly, at day 3 posttransfection, its levels were sustained in HeLa cells but had already begun to decline in the two hepatoma cell lines. To further ascertain that HCV indeed induced the expression of AP-1 transcripts, we performed a semiquantitative PCR for AP-1 using serial dilutions of the cDNA samples obtained from HepG2 cells. The results indicated that HCV-mediated induction of AP-1 transcripts was associated with a small increase of twofold over basal levels (Fig. 13B). These results
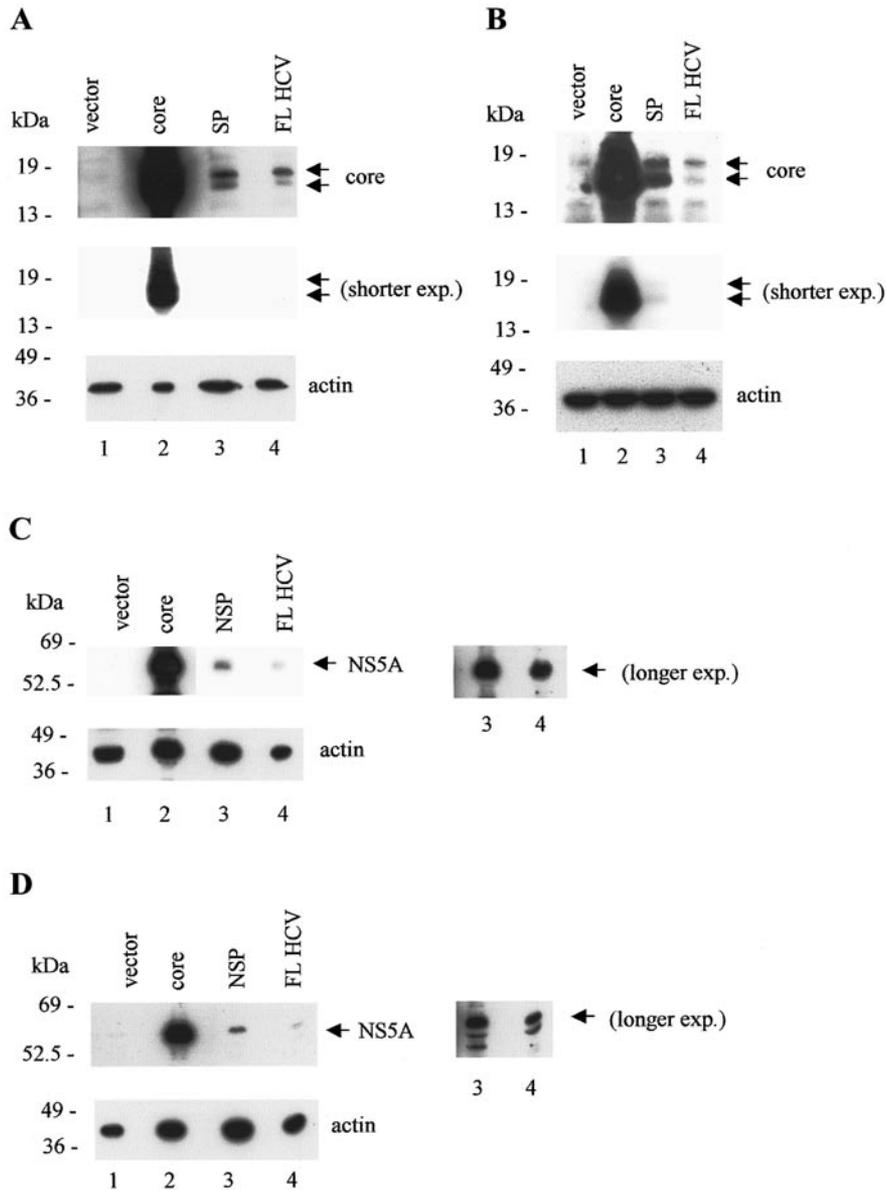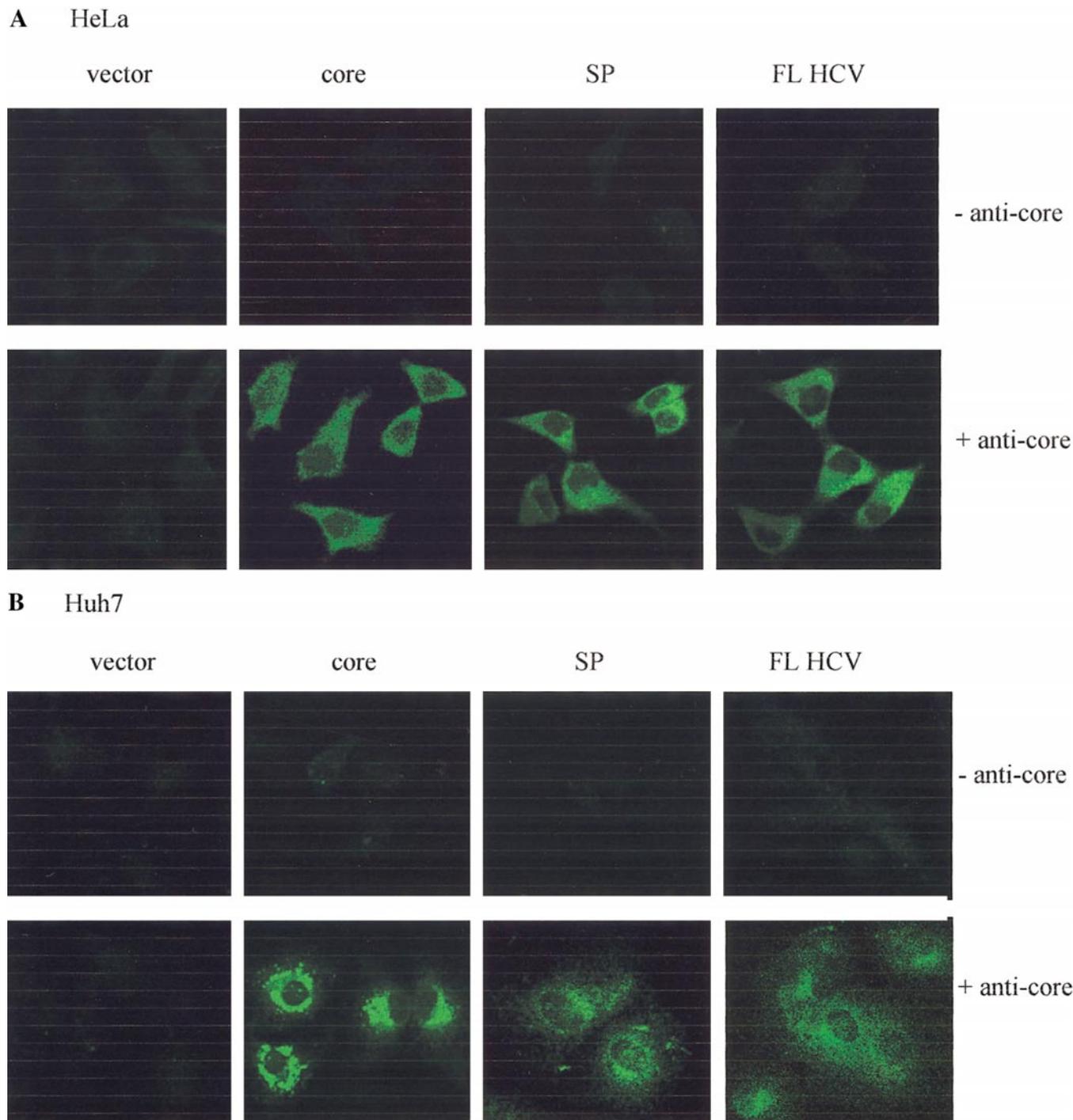
FIG. 11. (A and B) Expression of HCV core proteins in HeLa (A) and Huh7 (B) cells transiently cotransfected with phR181 and vector (lane 1), core (lane 2), structural proteins (SP, lane 3), and full-length (FL) HCV (lane 4) expression constructs. Cells were harvested at 35 h posttransfection. Cell lysates were subjected to luciferase assay (Fig. 9) and cell pellets for Western analyses. Pellets were denatured in 1× SDS–loading buffer and resolved on 12% SDS–PAGE gels and subjected to immunoblot analyses with rabbit polyclonal anticore antibodies as described under Materials and Methods. (C and D) Expression of HCV NS5A proteins in HeLa (C) and Huh7 (D) cells transiently cotransfected with phR181 and vector (lane 1), NS5A (lane 2), nonstructural proteins (NSP, lane 3), and full-length (FL) HCV (lane 4) expression constructs. Cells were harvested at 35 h posttransfection. Cell lysates were subjected to luciferase assay (Fig. 9) and cell pellets for Western analyses for NS5A as described in A and B. Arrows indicate the respective HCV proteins. Molecular masses in kilodaltons (kDa) of protein molecular weight markers are indicated on the left. Levels of HCV protein expressed were normalized against endogenous actin levels. A shorter exposure (exp.) of the Western blots of (A) and (B) and a longer of exposure of (C) and (D) are also shown.

showed that FL HCV could enhance the activity of AP-1 at two levels: the first by inducing the expression of its transcripts, and the second by increasing its binding activities to promoter sequences.

DISCUSSION

HCV causes persistent infection, chronic hepatitis in most infected individuals, which eventually progresses to cirrhosis and hepatocellular carcinoma (HCC). Spontaneous recovery following HCV infection is a relatively rare event. Although CD4^{+} and CD8^{+} positive T lymphocytes are believed to be important in viral clearance during the acute phase of viral infection (Koziel, 1997; Pape et al., 1999; Gruner et al., 2000), they are also involved in the pathogenesis of infection (Jin et al., 1997; Liaw et al., 1995; Tsai et al., 1997; reviewed in Koziel,

A HeLa

B Huh7

FIG. 12. Indirect immunofluorescence staining of HCV core proteins in HeLa (A) and Huh7 (B) cells transiently cotransfected with vector, or expression constructs for core, structural proteins (SP), and full-length (FL) HCV. Cells were harvested at 35 h posttransfection, permeabilized with 0.1% saponin, and immunostained as described under Materials and Methods. Cells are labeled with anticore antibody, 515S (bottom panels), or secondary antibody alone (top panels). Control vector-transfected cells gave little background staining, while core-expressing cells showed strong cytoplasm staining in HeLa cells (A) or perinuclear staining in Huh7 cells (B). Experiments repeated by permeabilization with 0.2% Triton X-100 gave similar results (data not shown).

1997; Tsai and Huang, 1997). Moreover, chronic hepatitis C infection is characterized by the presence of a large number of lymphocytes in the inflamed liver (Grabowska et al., 2001; reviewed in Valiante et al., 2000), which are implicated in liver damage during infection and as well in control of viral replication. These cells are clonotypically different from those of the periphery, suggesting specific compartmentalization of particular CD4^{+} T cell subsets
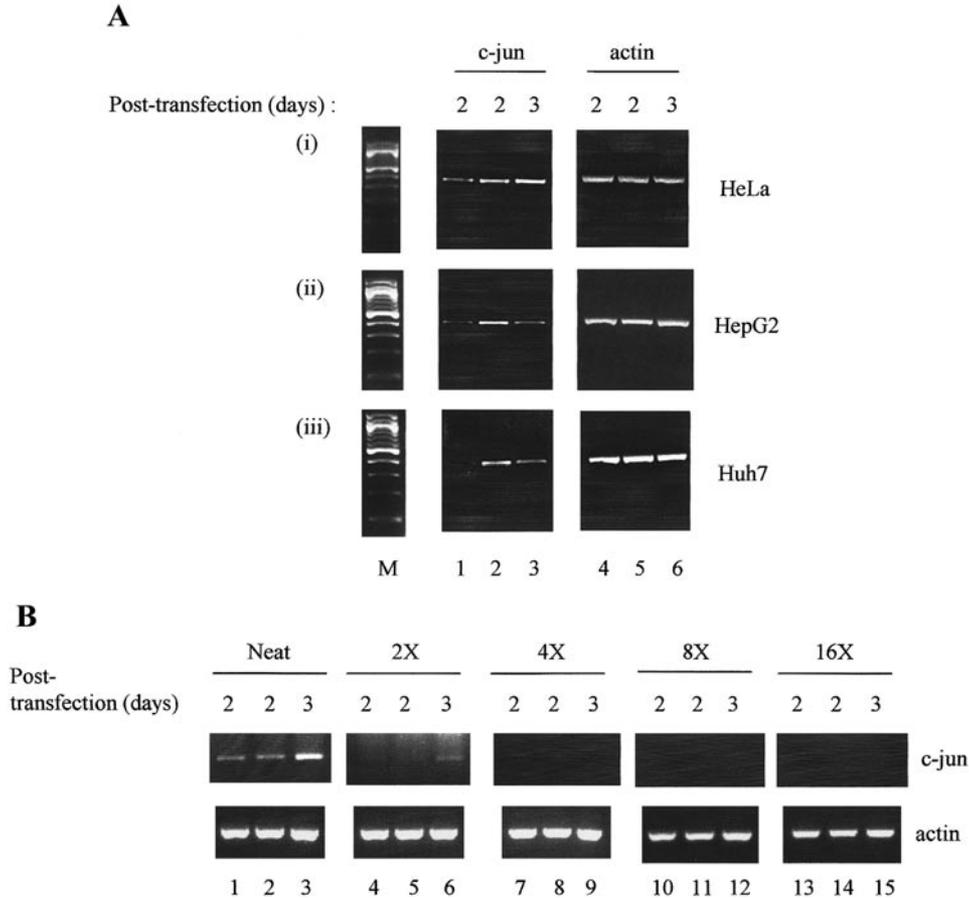
FIG. 13. (A) RT-PCR of c-*jun* transcripts in (i) HeLa, (ii) HepG2, and (iii) Huh7 cells transfected with pXJ(S1) at 2 (lane 2) and 3 (lane 3) days posttransfection. As a control, cells were transfected with vector pXJ41neo for 2 days (lane 1). RT-PCR was performed on total cellular RNA extracted from cells as described under Materials and Methods. Levels of endogenous actin mRNA (lanes 4–6) were used for normalization. (B) Semiquantitative detection of c-*jun* mRNA in HepG2 cells by RT-PCR. Cells were transfected with pXJ(S1) for 2 (lanes 2, 5, 8, 11, and 14) and 3 days (lanes 3, 6, 9, 12, and 15) or with vector pXJ41neo for 2 days (lanes 1, 4, 7, 10, and 13). Serial dilutions of cDNA samples (1:2, 1:4, 1:8, and 1:16, depicted as 2×, 4×, 8×, and 16×) were prepared and subjected to PCR as in (A). Levels of endogenous actin mRNA (iii) are shown.

in the liver (Minutello *et al.,* 1993). As was the case with hepatitis B virus (Kakimi *et al.,* 2001), migration to and preferential sequestration of $CD4^+$ and $CD8^+$ T cells in the HCV-infected liver is likely associated with the chemokines. In this study, we show that HCV up-regulates the expression of two CC chemokines, MCP-1 and RANTES. In both nonhepatic and hepatic cells, induction of transcripts for both genes was observed as early as 2 days posttransfection with a FL HCV genome (Fig. 2). Induction of transcripts led to increased production of these proteins (Fig. 3).

Further investigation revealed that the promoter activities of both MCP-1 and RANTES were enhanced by full-length HCV genome expression. Our transfection experiments showed that a 128-nt sequence immediately upstream of the translational start site of the hMCP-1 promoter (Shyy *et al.,* 1993; Li and Kolattukudy, 1994; Lim and Garzino-Demo, 2000) was sufficient to give optimal HCV-mediated gene activity in transfected HeLa and

Huh7 cells (Figs. 4A and 4B). We determined from EMSAs that transfection of full-length HCV genome specifically induced the binding of AP-1 activities to the 128-nt promoter sequence (nt −122), in Huh7 cells, while SP-1 (nt −115) and NF-1 (nt −70) binding activities were responsible for its constitutive expression (Fig. 5). Supershifts performed with SP-1 and AP-1 antibodies confirm this finding (Fig. 5). The activity of an MCP-1 promoter construct with additional upstream sequences (nt 129–213) was only marginally increased as compared to the 128-nt promoter sequence in the presence of HCV (Figs. 4A and 4B). Thus, it appeared that the upstream AP-1 and NF-κB site at nt −150 and −137, respectively, did not play a significant role in HCV-mediated activation of hMCP-1. This modality of activation differs from that which we characterized in HIV-1 Tat-mediated up-regulation of hMCP-1 (Lim and Garzino-Demo, 2000), where SP-1, AP-1, as well as NF-κB activities were involved, but instead is similar to the reported activation of hMCP-1 by

TPA, in which only the AP-1-binding elements were important for its activation (Shyy et al., 1993; Li and Kolattukudy, 1994).

In transfection studies performed with RANTES deletion constructs, a 181-nt sequence immediately upstream of the translational start site of the RANTES promoter (Nelson et al., 1993, 1996) was sufficient to give maximal HCV-mediated gene activity in transfected HeLa and Huh7 cells (Figs. 4C and 4D). This level of activation is comparable to those in studies carried out in the T lymphoma cell line, Hut78 (Nelson et al., 1993), in PHA-activated PBLs (Nelson et al., 1996), and dengue-infected cells (Lin et al., 2000). Although three AP-1 sites (−402, −420, −429) are located within the RANTES promoter region (Nelson et al., 1993), our studies indicated that they did not play a role in HCV-mediated induction of RANTES. We determined from EMSAs performed with extracts from Huh7 cells that factors binding to the A/B site in this region were mainly responsible for mediating basal RANTES promoter activity (Fig. 7). HCV further augmented the binding of these factors at this sequence (Fig. 7). Interestingly, we observed that NF-κB was involved in the basal expression of RANTES through binding at A/B site, and HCV increased its binding to this element (Fig. 7). Nevertheless, binding of other unknown factors also appeared to be enhanced. Recently, dengue-virus 2 was also shown to up-regulate RANTES promoter activity through binding of NF-IL6 and undefined factor(s) at regions E and A/B, respectively, in hRAN181 (Lin et al., 2000). However, we failed to observe any HCV-mediated increase in the binding of NF-IL6 to hRAN181 (which suggests a different regulation of the RANTES promoter by Dengue-virus 2 and HCV), although we found that NF-IL6 was involved in mediating basal RANTES expression (Fig. 6). The identity of the HCV-induced A/B binding factor is currently being investigated.

Thus although the full-length HCV genome we have constructed was capable of inducing NF-κB and AP-1 activities to similar extents (Fig. 8), these factors participate to different degrees in the activation of different CC chemokine genes. The reason for this phenomenon is unknown, but may be due to a difference in the affinity of AP-1 and NF-κB for their respective binding elements on the MCP-1 and RANTES promoters to their ability to cooperate with adjacent binding factors on these promoters or to cell type-specificity.

Several groups have reported that AP-1 activities are induced by the HCV core (Shrivastava et al., 1998; Kato et al., 2000) and NS5A (Polyak et al., 2001). Similarly, induction of NF-κB-binding activities by HCV core (Shrivastava et al., 1998; Marusawa et al., 1999; Kato et al., 2000; Tai et al., 2000; Watashi et al., 2001; Yoshida et al., 2001) and NS5A (Gong et al., 2001; Polyak et al., 2001) proteins have also been described. Nevertheless, it remains possible that other viral proteins are involved either directly or indirectly. Our experiments indicated that NS5A was able

to activate both AP-1 and NF-κB activities in HeLa and Huh7 cells (Figs. 9 and 10, Table 1). Similarly, it activates both MCP-1 and RANTES promoter sequences in these two cell lines. Other nonstructural HCV proteins did not appear to activate either AP-1 or NF-κB, as an expression construct bearing all the nonstructural proteins was not significantly more active than the expression construct for NS5A alone. Nevertheless, in Huh7 cells, other nonstructural protein(s) may be able to activate RANTES in a NF-κB-independent manner (Table 1).

In contrast, HCV core activated AP-1 and NF-κB specifically in HeLa cells (Figs. 9 and 10, Table 1). A strong suppression of both AP-1 and NF-κB activities was observed in Huh7 cells (Figs. 9 and 10, Table 1). Thus, not surprisingly, core failed to activate the promoter elements of both MCP-1 and RANTES genes in Huh7 cells but strongly augmented their binding activities in HeLa cells (Figs. 9 and 10, Table 1). A similar suppressive effect of core on AP-1 and NF-κB was observed in another hepatoma cell line, HepG2 (data not shown). While our findings concur with other reports of core-mediated induction of NF-κB activities in HeLa cells (Shrivastava et al., 1998; Marusawa et al., 1999; Kato et al., 2000; Yoshida et al., 2001), they appear to contradict the study of You et al. (1999), who found increased NF-κB binding activities in stable core-expressing HeLa and Huh7 cells. Instead, our observations are more consistent with those of Shrivastava et al. (1998), who reported that core can suppress the DNA-binding activities of NF-κB induced by cytokines in MCF cells.

It has been reported that truncated core proteins lacking 20 or more amino acids from the C-terminal end translocate to the nucleus (Suzuki et al., 1995; Lo et al., 1996; Watashi et al., 2001) and do not activate NF-κB (Watashi et al., 2001). Yet, in our hands, two forms of processed core with molecular weight of less than 19 kDa were consistently found in the cytoplasm of transfected HeLa and Huh7 when expressed either alone or together with other HCV structural and nonstructural proteins (Figs. 11 and 12). At the same time, these isoforms of core display different effects on gene regulation in these two cell types. Nevertheless, core could be sublocalized to different compartments in the cytoplasm of HeLa and Huh7 cells. In the former, it appears to be evenly distributed in the cytoplasm, while in the latter, it appears to be localized mainly to the perinuclear region (Fig. 12). Furthermore, a construct bearing all the structural proteins persistently failed to activate AP-1 and NF-κB in both HeLa and Huh7 cells (Table 1), suggesting that E1 and E2 proteins may interact with core (such as for viral assembly) and prevent/reduce its ability to activate the two transcription factors. Indeed in support of this hypothesis, interaction between E1 and core have been described (Lo et al., 1996).

From these results, we postulate that following HCV infection in the liver, NS5A, rather than core, is important

in mediating intracellular events, such as through the induction of DNA-binding activities of cellular transcriptional factors such as AP-1 and NF-κB. In addition, it is possible that other HCV nonstructural proteins may also have gene-regulation properties (Table 1; Kato *et al.,* 2000). Remarkably, we observed that c-*jun* transcription is also enhanced by FL HCV (Fig. 13). Thus it appears that HCV-mediated up-regulation of AP-1 activities occurs at two levels: during transcription and in posttranslation.

HCV is known to cause not only acute and chronic liver disease, but also immunological and hematologic disorders, such as autoantibody production, mixed cryoglobulinemia, and B cell lymphoproliferation (Killenberg, 2000). Moreover, HCV has also been demonstrated to infect and replicate in peripheral blood mononuclear cells (PBMCs) (Gabrielli *et al.,* 1994), which may be responsible for the various HCV-associated extrahepatic manifestation. In support of this, both positive and negative strands of the HCV RNA can be detected in B-, T-lymphocytes, monocytes, and polymorphonuclear leukocytes (PML) in HCV-positive patients (Crovatto *et al.,* 2000; Mellor *et al.,* 1998). Our findings here suggest that HCV may induce the migration of monocytes, dendritic, NK, and/or T cells into the liver through the induction of MCP-1 and RANTES production in HCV-infected hepatocytes, thus possibly contributing to the infection of PBMCs, and extrahepatic manifestations. This hypothetical model is substantiated by reports that HCV-specific B cells (Zehender *et al.,* 1997; Sansonno *et al.,* 1998), T cells (Minutello *et al.,* 1993; Crispe *et al.,* 2000), NK, and TCRγ/δ+ cells (Nuti *et al.,* 1998) accumulate in the liver of infected patients. Moreover, HCV induction of CC chemokine expression may contribute to Fas-mediated killing of the infiltrating T cells (Crispe *et al.,* 2000). CD8$^+$ T cells have also been reported to disappear following the acute phase of HCV infection resulting in viral persistence (Lechner *et al.,* 2000). Additionally, induction of CC chemokine may result in T cell activation intrahepatically (Grabowska *et al.,* 2001), causing liver damage and possibly hepatocarcinogenesis (Liaw *et al.,* 1995; Jin *et al.,* 1997; Tsai *et al.,* 1997; Pape *et al.,* 1999; Grabowska *et al.,* 2001). Understanding the mechanisms of activation of CC chemokines such as MCP-1 and RANTES by HCV could provide some insights into better management and control of HCV-associated diseases.

MATERIALS AND METHODS

Construction of HCV-S1 cDNA clones encoding HCV 5'NCR and structural proteins

The region spanning the 5'NCR to the end of the p7 (from nt −276 to 2461) was PCR amplified using clones C and D (Lim *et al.,* 2001) as templates with the primers H2 and H12 (Lim *et al.,* 2001). The resulting 2.7-kb PCR product and a 600-bp PCR product comprising the NS2

cDNA (from nt 1 to 346) were used as templates in a second round of PCR to produce a 3.3-kb DNA fragment. This PCR product and clone A (comprising nt −341 to −72 of the HCV 5'NCR) (Lim *et al.,* 2001) were used as templates in a third round of PCR to generate clone J (nt −341 to 2461). The PCR conditions were previously described (Lim *et al.,* 2001). Clone J was digested with *Eco*RI and recloned into pcDNA3.1(+) from Invitrogen (Carlsbad, CA) and pXJ41neo (Zheng *et al.,* 1992) to generate pcDNA3(SP) and pXJ41(SP), respectively.

Construction of HCV-S1 cDNA clones encoding HCV nonstructural proteins and 3′ UTR

The region spanning NS3 to NS5A (from nt 3079 to 7328) was obtained by simultaneous insertion of a 1.844-kb *Bam*HI/*Bmr*I fragment from clone F (Lim *et al.,* 2001) and a 2.4-kb *Bmr*I/*Eco*RV fragment from clone G (Lim *et al.,* 2001), into pKSII (+/−) (Stratagene, Heidelberg, Germany) digested with *Bam*HI and *Eco*RV. The resulting clone was digested with *Xba*I and *Bsr*GI and inserted with a 0.9-kb *Xba*I/*Bsr*GI fragment containing the NS2 ORF from clone E (Lim *et al.,* 2001) to produce clone K (comprising nt 2428−7328). To obtain the region spanning nt 7200 to 9268, clones H and I (Lim *et al.,* 2001) were used as templates in a PCR reaction with primers H22 and H26 (Lim *et al.,* 2001) to generate clone L. Clones K and L were double-digested with *Bcl*I and *Eco*RV and ligated together to generate clone M (comprising nt 2428−9268). Clone M was digested with *Not*I and *Xho*I and recloned into pcDNA3.1(+) and pXJ41neo to generate pcDNA3(NSP) and pXJ41(NSP), respectively.

Construction of full-length cDNA clones of HCV-S1

Clones J and M were double-digested with *Csp*I and *Xba*I and ligated together to generate the full-length HCV genome of HCV-S1 in pKSII(+/−) designated pKSII(S1). To generate the full-length clone in pcDNA3.1(+), the EcoRV/BsrGI fragment from pKSII(S1) was ligated to the pcDNA3(NSP) digested with the same enzymes. To create the full-length clone in pXJ41neo, the same fragment was cloned into the blunt *Not*I/*Bsr*GI site in pXJ41(NSP). These constructs were designated pcDNA3(S1) and pXJ41(S1), respectively.

Sequence analysis

DNA sequencing on all constructs created was carried out in the core facility at the Institute of Molecular and Cell Biology. Used were 200 ng of the double-stranded templates and 10 ng of primers with the Taq DyeDeoxy terminator cycle sequencing kit and the automated DNA sequencer 373 from PE Applied Biosystems (Foster City, CA).

TABLE 1

Summary of the HCV-Mediated Induction of the Various Reporter Promoter Constructs in the Cell Lines HeLa and Huh7

	Folds of increase in HeLa (X)				Folds of increase in Huh7 (X)			
	NF-κB	phR181	AP-1	phMCP128	NF-κB	phR181	AP-1	phMCP128
Vector	1.0	1.0	1.0	1.0	1.0	1.0	1.0	1.0
Core	11.4	5.2	3.0	4.3	0.4	0.3	0.2	0.4
NS5A	2.6	2.8	2.5	3.0	2.4	2.7	2.3	2.5
SP	0.9	2.0	1.0	2.5	1.6	2.0	1.8	2.0
NSP	2.9	3.9	3.6	3.5	3.2	6.8	3.5	4.5
FL HCV	2.6	5.6	4.6	3.5	3.1	6.8	4.2	3.8

Note. The results are represented as folds of increase of luciferase values over basal levels obtained from cotransfection with empty vector.

Cells and cell culture

The human embryonic kidney cell line, 293, bearing the large T antigen from SV40 (293T), the human epitheloid cervical carcinoma cell line HeLa, and human hepatoma cell line, HepG2, were purchased from American Type Cell Collection. The human hepatoma cell line, Huh7, was obtained from Japan Health Sciences Foundation (Chou-ku, Osaka). The cells were cultured in Eagles' MEM containing 2 mM L-glutamine, 1.5 g/L sodium bicarbonate, 0.1 mM nonessential amino acids, 1 mM sodium pyruvate, and 10% fetal bovine serum and maintained at 37°C in 5% CO_2.

Cell transfections

Transfection experiments were performed using Effectene transfection reagent from Qiagen (Valencia, CA). Cells (1.5×10^5) were plated into six-well tissue culture plates 14–18 h before transfection. One microgram of plasmid DNA in 150 μl EC buffer was mixed with 8 μl of enhancer and the mixture was allowed to stand at room temperature for 2–5 min. Effectene transfection reagent (25 μl) was added and the mixture was incubated at room temperature for another 5–10 min. Cells were washed once with PBS and added with DNA-Effectene mixture diluted in 2 ml of complete growth medium. The cultures were incubated at 37°C and 5% CO_2 for 4–6 h,

after which the medium was aspirated and the cells washed again. Added to the cells was 2.5 ml fresh complete medium and incubation was continued for another 48–120 h, after which cells were harvested for RNA isolation, Western analyses, or luciferase assays.

RNA extraction

Transfected cells were harvested by trypsin treatment and washed twice in PBS. The cell pellet was lysed with 1.2 ml of the Trizol reagent from Gibco-BRL (Gaithersburg, MD). The mixture stood at room temperature for 5 min; 0.35 ml of chloroform was added, and the mixture was inverted for 20 s. It was incubated for another 5 min and centrifuged at 12,000 rpm for 20 min. The upper phase was transferred to a new Eppendorf tube; 0.8 ml of isopropanol was added, and the mixture was mixed by inversion again. The tube was left at room temperature for 5 min, after which it was spun again at 12,000 rpm for 20 min at 4°C. The RNA pellet was air-dried and resuspended with 50 μl of DEPC-treated water.

RT-PCR

Primers for RT-PCR to detect MCP-1, RANTES, c-*jun,* and actin are listed in Table 2. To detect chemokine mRNA, 2.5 μl of the RNA isolated from transfected cells was reverse transcribed at 42°C for 30 min using ran-

TABLE 2

Sequences of RT-PCR Primers

Primers	Sequence (5'–3')	Location
MCP-1 FOR	AGTCTCTGCCGCCCTTCTGTG	nt 59–81
MCP-1 REV	GAATCCTGAACCCACTTCTGCT	nt 288–310
RANTES FOR	ACGCCTCGCTGTCATCCTCATT	nt 44–65
RANTES REV	ACTCTCCATCCTAGCTCATCTC	nt 291–312
c-*jun* FOR	TTAACAGTGGGTGCCAACTCATGCTAACGC	nt 2207–2237
c-*jun* REV	GAGATCGAATGTTAGGTCCATGCAGTTCTTG	nt 2583–2552
GAPDH FOR	CTGAGAACGGGAAGCTTGTCATCAA	nt 288–312
GAPDH REV	CGTCTAGCTCAGGGATGACCTTGC	nt 774–756

dom hexanucleotides and 200 U MMLV RT (New England Biolabs, Inc., Beverly, MA). PCR conditions were as follows: 95°C for 3 min, followed by 30–40 cycles of 95°C for 1 min, 50°C for 1 min, 72°C for 1 min, and a final extension 72°C for 8 min. Amplified products were visualized by ethidium bromide staining in a 3% agarose gel.

Luciferase assays

The plasmid pGL2-Basic was purchased from Promega (Madison, WI), while pAP1-Luc and pNF-κB plasmids were obtained from Stratagene. The two deletion constructs of the human MCP-1 (hMCP-1) promoter, phMCP213 and phMC128, which covered from nts −213 to +6 and −128 to +6, respectively, were previously described (Lim and Garzino-Demo, 2000). Those for the human RANTES promoter, phR961 and phR181, covering the regions from nt −961 to +6 and −181 to +6, were also previously described (Nelson *et al.,* 1993, 1996) and kindly provided by Alan M. Krensky (Stanford University, CA). Luciferase activity was measured using the dual-luciferase reporter assay system from Promega. Following a 35–48 h incubation period, cells were washed twice with PBS and lysed with 150 μl of reporter lysis buffer. The lysate was allowed to stand at room temperature for 10–15 min and collected into 1.5 ml Eppendorf tubes. These were spun for 1 min in a microfuge and 10 μl of each lysate was mixed with 100 μl buffer and measured for luciferase activities in a Turner luminometer (Turner Designs, Sunnydale, CA) over an integration period of 15 s. Values obtained were normalized with the levels of renilla luciferase in the cell lysates. Less than 20% variation was observed between samples.

Nuclear extracts and electrophoretic mobility shift assays

Nuclear extracts were prepared from 10^7 cells as described previously (Lim and Garzino-Demo, 2000). Protein concentration was determined with the bicinchoninic acid (BCA) protein assay from Pierce (Rockford, IL) and determined to be between 3–10 μg/ml. The DNA fragment from −128 to +6 of the hMCP-1 promoter was excised from the plasmid phMCP128 with *Nhe*I and *Bgl*II and that from −181 to +6 of the hRANTES promoter was excised from the plasmid phRAN181 with *Xba*I and *Pst*I. Both DNA fragments were filled in using [α-^{32}P]dCTP (New England Biolabs) and Klenow fragment. Oligonucleotides containing NF-IL6 (nt −164) and A/B site (nt −131 to −103) (Nelson *et al.,* 1996) were annealed and end-labeled with γ-^{32}P-ATP and T4 kinase. Mobility shift electrophoresis assay mixtures contained 0.25 ng of ^{32}P-labeled DNA fragment or double-stranded oligonucleotides (15,000 cpm), 10 mM HEPES at pH 7.9, 1 mM dithiothreitol, 1 mM EDTA, 0.5 mM MgCl$_2$, 5% glycerol, 0.5 μg poly(dI-dC), 0.1 μg sonicated salmon sperm DNA, and 4 μg of nuclear extract. The binding reactions were incubated on ice for 20 min and electrophoresed through 5% native polyacrylamide gels in 25 mM Tris borate/0.5 mM EDTA at 270 V for 2–3 h. The gels were dried down and exposed to X-ray films for 12–16 h at −70°C. Competition assays were performed with 100-fold molar excess cold DNA fragments from regions −128 to +6 of hMCP promoter, and region −181 to +6 of hRANTES promoter or double-stranded oligonucleotides containing SP1, AP1, NF-κB, NF1 (Lim and Garzino-Demo, 2000), and NF-IL6 and A/B site (Nelson *et al.,* 1996) binding elements. Supershifts were performed with by preincubation of nuclear extracts with 200 ng of Sp1, AP-1, p50, or p65 polyclonal antibodies from Santa Cruz Biotechnology (Santa Cruz, CA) for 10 min and preincubating the reaction mixture as described above.

Western blot analysis

Cell lysates were resolved on a 10 or 12% sodium dodecyl sulphate (SDS)–polyacrylamide gel, transferred to a nitrocellulose membrane, blocked with 5% nonfat skim milk in PBS-T, and reacted with primary antibodies followed by anti-mouse, anti-rabbit, or anti-human antibodies conjugated with horseradish peroxidase (Sigma, St. Louis, MO). Membrane-bound antibodies were detected with the SuperSignal west pico chemiluminescence substrate kit (Pierce). The E2 (H52) monoclonal antibody which recognizes a conformation-independent epitope was a kind gift from Jean Dubuisson (Institut de Biologie de Lille and Institut Pasteur de Lille, Lille Cedex, France). The monoclonal antibodies for E1 and NS-3 were purchased from Austral Biologicals (San Ramon, CA), and Devaron, Inc. (Dayton, NJ), respectively, and those for NS-4B, and -5A were from Biodesign International (Kennebunk, ME). To detect core and NS5B, sera from HCV-infected patients were used at dilutions of 1:40−1:100. To screen for sera specific against core and NS5B, we carried out Western analyses with the patient sera on 293T cells transiently transfected with expression constructs of core or NS5B. A total of 15 patient sera samples was tested, three of which were found to react to NS5B, and at least six were found to react to core (data not shown). Rabbit polyclonal anticore antibodies generated with recombinant core protein (aa 1−140) were also used for analyses.

Intracellular chemokine staining by flow cytometry

Cells were harvested 2−3 days posttransfection, washed in PBS, and resuspended at 1 × 10^6 cells/ml. Cells were added with 1 vol of 4% formaldehyde/PBS and incubated at RT for 20 min, followed by washing in PBS. The cells were spun down and the pellet resuspended in 0.5 μg PE-conjugated mouse anti-human RANTES or MCP-1 monoclonal antibody (PharMingen, San Diego, CA) in PBS containing 0.5% saponin, 0.5% bovine serum albumin, and 0.02% Na azide. Incubation was carried at

RT for 20 min after which the cells were washed and analyzed on a Becton–Dickinson FACScalibur flow cytometer (San Jose, CA). Live cells were gated and a total of 10,000 events was collected per analysis.

Indirect immunofluorescence

Cells grown overnight on coverslips were transfected for 35 h, fixed in 4% paraformaldehyde, and permeabilized with 0.1% saponin. They were stained with anticore antibody, 515S (diluted 1:100, a kind gift from Prof. Michinori Kohara, The Tokyo Metropolitan Institute of Medical Science, Tokyo, Japan) in 2% BSA in PBS, followed by fluorescence isothiocyanate-conjugated anti-mouse antibody (Sigma). Cells were washed with PBS between steps. Coverslips were mounted and immunofluorescence microscopy analyses performed with a MRC1024 (Bio-Rad) confocal laser scanning system.

ACKNOWLEDGMENTS

REFERENCES

Aizaki, H., Aoki, Y., Harada, T., Ishii, K., Suzuki, T., Nagamori, S., Toda, G., Matsuura, Y., and Miyamura, T. (1998). Full length complementary DNA of hepatitis C virus genome from an infectious blood sample. *Hepatology* **27,** 621–627.

Alter, H. J., Purcell, R. H., Shih, J. W., Melpolder, J. C., Houghton, M., Choo, Q. L., and Kuo, G. (1989). Detection of antibody to hepatitis C virus in prospectively followed transfusion recipients with acute and chronic non-A, non-B hepatitis. *N. Engl. J. Med.* **321,** 1491–1500.

Bertolini, L., Iacovacci, S., Ponzetto, A., Gorini, G., Bataglia, M., and Carloni, G. (1993). The human bone marrow-derived B-cell line susceptible to hepatitis C virus infection. *Res. Virol.* **144,** 281–285.

Blight, K. J., Kolykhalov, A. A., and Rice, C. M. (2000). Efficient initiation of HCV RNA replication in cell culture. *Science* **290,** 1972–1974.

Chen, C. J., Liao, S. L., Kuo, M. D., and Wang, Y. M. (2000). Astrocytic alteration induced by Japanese encephalitis virus infection. *Neuroreport* **11,** 1933–1937.

Choo, Q. L., Kuo, G., Weiner, A. J., Overly, L. R., Bradley, D. W., and Houghton, M. (1989). Isolation of a cDNA clone derived from a blood-borne non-A, non-B hepatitis genome. *Science* **244,** 359–362.

Choo, Q. L., Richman, K. H., Hau, J. H., Berger, K., Lee, C., Dong, C., Gallegos, C., Coit, D., Medina, S. R., and Barr, P. J. (1991). Genetic organization and diversity of the hepatitis C virus. *Proc. Natl. Acad. Sci.* **88,** 2451–2455.

Crispe, I. N., Dao, T., Klugewitz, K., Mehal, W. Z., and Metz, D. P. (2000). The liver as a site of T-cell apoptosis: Graveyard, or killing field? [Review]. *Immunol. Rev.* **174,** 47–62.

Crovatto, M., Pozzato, G., Zorat, F., Pussini, E., Nascimben, F., Baracetti, S., Grando, M. G., Mazzaro, C., Reitano, M., Modolo, M. L., Martelli, P., Spada, A., and Santini, G. (2000). Peripheral blood neutrophils from

hepatitis C virus-infected patients are replication sites of the virus. *Haematologica* **85,** 356–361.

Dammacco, F., Sansonno, D., Piccoli, C., Racanelli, V., D'Amore, F. P., and Lauletta, G. (2000). The lymphoid system in hepatitis C virus infection: Autoimmunity, mixed cryoglobulinemia, and Overt B-cell malignancy. *Semin. Liver Dis.* **20,** 143–157.

Gabrielli, A., Manzin, A., Candela, M., Caniglia, M. L., Paolucci, S., Danieli, M. G., and Clementi, M. (1994). Active hepatitis C virus infection in bone marrow and peripheral blood mononuclear cells from patients with mixed cryoglobulinaemia. *Clin. Exp. Immunol.* **97,** 87–93.

Gong, G., Waris, G., Tanveer, R., and Siddiqui, A. (2001). Human hepatitis C virus NS5A protein alters intracellular calcium levels, induces oxidative stress, and activates STAT-3 and NF-kappa B. *Proc. Natl. Acad. Sci. USA* **98,** 9599–9604.

Grabowska, A. M., Lechner, F., Klenerman, P., Tighe, P. J., Ryder, S., Ball, J. K., Thomson, B. J., Irving, W. L., and Robins, R. A. (2001). Direct *ex vivo* comparison of the breadth and specificity of the T cells in the liver and peripheral blood of patients with chronic HCV infection. *Eur. J. Immunol.* **31,** 2388–2394.

Gruner, N. H., Gerlach, T. J., Jung, M. C., Diepolder, H. M., Schirren, C. A., Schraut, W. W., Hoffmann, R., Zachoval, R., Santantonio, T., Cucchiarini, M., Cerny, A., and Pape, G. R. (2000). Association of hepatitis C virus-specific CD8+ T cells with viral clearance in acute hepatitis C. *J. Infect. Dis.* **181,** 1528–1536.

Gupta, M., Mahanty, S., Ahmed, R., and Rollin, P. E. (2001). Monocyte-derived human macrophages and peripheral blood mononuclear cells infected with ebola virus secrete MIP-1alpha and TNF-alpha and inhibit poly-IC-induced IFN-alpha *in vitro*. *Virology* **284,** 20–25.

Haeberle, H. A., Kuziel, W. A., Dieterich, H. J., Casola, A., Gatalica, Z., and Garofalo, R. P. (2001). Inducible expression of inflammatory chemokines in respiratory syncytial virus-infected mice: Role of MIP-1alpha in lung pathology. *J. Virol.* **75,** 878–890.

Harada, S., Watanabe, Y., Takeuchi, K., Suzuki, T., Katayama, T., Takebe, Y., Saito *et al.* (1991). Expression of processed core protein of hepatitis C virus in mammalian cells. *J. Virol.* **65,** 3015–3021.

Hijikata, M., Kato, N., Ootsuyama, Y., Nakagawa, M., and Shimotohno, K. (1991). Gene mapping of the putative structural region of the hepatitis C virus genome. *Proc. Natl. Acad. Sci. USA* **88,** 5547–5555.

Houghton, M., Weiner, A., Han, J., Kuo, G., and Choo, Q. L. (1991). Molecular biology of the hepatitis C viruses: Implications for diagnosis, development and control of viral disease. *Hepatology* **14,** 381–388.

Hussy, P., Langen, H., Mous, J., and Jacobson, H. (1996). Hepatitis C virus core protein: Carboxy-terminal boundaries of two processed species suggest cleavage by a signal peptide peptidase. *Virology* **224,** 93–104.

Iacovacci, S., Sargiacomo, M., Parolini, I., Ponzetto, A., Peschle, C., and Carloni, G. (1993). Replication and multiplication of hepatitis C virus genome in human fetal liver cells. *Res. Virol.* **144,** 275–279.

Ikeda, M., Sugiyama, K., Mizutani, T., Tanaka, T., Tanaka, K., Sekihara, H., Shimotohno, K., and Kato, N. (1998). Human hepatocyte clonal cell lines that support persistent replication of hepatitis C virus. *Virus Res.* **56,** 157–167.

Ito, T., Mukaigawa, J., Zuo, J., Hirabayashi, Y., Mitamura, K., and Yasui, K. (1996). Cultivation of hepatitis C virus in primary hepatocyte culture from patients with chronic hepatitis C results in release of high titer infectious virus. *J. Gen. Virol.* **77,** 1043–1054.

Jin, Y., Fuller, L., Carreno, M., Zucker, K., Roth, D., Esquenazi, V., Karatzas, T., Swanson, S. J., 3rd, Tzakis, A. G., and Miller, J. (1997). The immune reactivity role of HCV-induced liver infiltrating lymphocytes in hepatocellular damage. *J. Clin. Immunol.* **17,** 140–153.

Kakimi, K., Lane, T. E., Chisari, F. V., and Guidotti, L. G. (2001). Cutting edge: Inhibition of hepatitis B virus replication by activated NK T cells does not require inflammatory cell recruitment to the liver. *J. Immunol.* **15,** 167:6701–6705.

Kato, N., Yoshida, H., Kioko, Ono-Nita, S., Kato, J., Goto, T., Otsuka, M., Lan, K., Matsushima, K., Shiratori, Y., and Omata, M. (2000). Activation of intracellular signaling by hepatitis B and C viruses: C-viral core is the most potent signal inducer. *Hepatology* 32, 405–412.

Killenberg, P. G. (2000). Extrahepatic manifestations of chronic hepatitis C. *Semin. Gastrointest. Dis.* 11, 62–68.

Koziel, M. J. (1997). The role of immune responses in the pathogenesis of hepatitis C virus infection. *J. Viral Hepat.* 4(Suppl. 2), 31–41.

Lanford, R. E., Sureau, C., Jacob, J. R., White, R., and Fuerst, T. R. (1994). Demonstration of *in vitro* infection of hepatocytes with hepatitis C virus using strand-specific RT/PCR. *Virology* 202, 606–614.

Lechner, F., Gruener, N. H., Urbani, S., Uggeri, J., Santantonio, T., Kammer, A. R., Cerny, A., Phillips, R., Ferrari, C., Pape, G. R., and Klenerman, P. (2000). CD8+ T lymphocyte responses are induced during acute hepatitis C virus infection but are not sustained. *Eur. J. Immunol.* 30, 2479–2487.

Leonard, E. J., and Yoshmura, T. (1990). Human monocyte chemoattractant protein-1 (MCP-1). *Immunol. Today* 11, 97–101.

Li, Y.-S., and Kolattukudy, P. E. (1994). Functional role of the cis-acting elements in human monocyte chemotactic protein-1 gene in the regulation of its expression by phorbol ester in human glioblastoma cells. *Mol. Cell. Biochem.* 141, 121–128.

Liaw, Y. F., Lee, C. S., Tsai, S. L., Liaw, B. W., Chen, T. C., Sheen, I. S., and Chu, C. M. (1995). T-cell-mediated autologous hepatocytotoxicity in patients with chronic hepatitis C virus infection. *Hepatology* 22, 1368–1373.

Lim, S. P., and Garzino-Demo, A. (2000). The human immunodeficiency virus type 1 Tat protein up-regulates the promoter activity of the beta-chemokine monocyte chemoattractant protein 1 in the human astrocytoma cell line U-87 MG: Role of SP-1, AP-1, and NF-kappaB consensus sites. *J. Virol.* 74, 1632–1640.

Lim, S. P., Khu, K. L., Hong, W. J., Tay, A., Ting, A. E., Lim, S. G., and Tan, Y. H. (2001). Identification and molecular characterisation of the complete genome of a Singapore isolate of hepatitis C virus: Sequence comparison with other strains and phylogenetic analysis. *Virus Genes* 23, 89–95.

Lin, Y. L., Liu, C. C., Chuang, J. I., Lei, H. Y., Yeh, T. M., Lin, Y. S., Huang, Y. H., and Liu, H. S. (2000). Involvement of oxidative stress, NF-IL-6, and RANTES expression in dengue-2-virus-infected human liver cells. *Virology* 276, 114–126.

Lo, S. Y., Selby, M. J., and Ou, J. H. (1996). Interaction between hepatitis C virus core protein and E1 envelope protein. *J. Virol.* 70, 5177–5182.

Lo, S. Y., Masiarz, F., Hwang, S. B., Lai, M. M., and Ou, J. H. (1995). Differential subcellular localization of hepatitis C virus core gene products. *Virology* 213, 455–461.

Lohmann, V., Korner, F., Koch, J. O., Herian, U., Theilmann, L., and Bartenschlager, R. (1999). Replication of subgenomic hepatitis C virus RNAs in a hepatoma cell line. *Science* 285, 110–113.

Marusawa, H., Hijikata, M., Chiba, T., and Shimotohno, K. (1999). Hepatitis C virus core protein inhibits Fas- and tumor necrosis factor alpha-mediated apoptosis via NF-kappaB activation. *J. Virol.* 73, 4713–4720.

Matikainen, S., Pirhonen, J., Miettinen, M., Lehtonen, A., Govenius-Vintola, C., Sareneva, T., and Julkunen, I. (2000). Influenza A and sendai viruses induce differential chemokine gene expression and transcription factor activation in human macrophages. *Virology* 276, 138–147.

Matsura, Y., Harada, S., Suzuki, R., Watanabe, Y., Inoue, Y., Saito, and Miyamura, T. (1992). Expression of processed envelope protein hepatitis C virus in mammalian and insect cells. *J. Virol.* 66, 1425–1431.

Mellor, J., Haydon, G., Blair, C., Livingstone, W., and Simmonds, P. (1998). Low level or absent *in vivo* replication of hepatitis C virus and hepatitis G virus/GB virus C in peripheral blood mononuclear cells. *J. Gen. Virol.* 79, 705–714.

Minutello, M. A., Pileri, P., Unutmaz, D., Censini, S., Kuo, G., Houghton, M., Brunetto, M. R., Bonino, F., and Abrignani, S. (1993). Compart-

mentalization of T lymphocytes to the site of disease: Intrahepatic CD4+ T cells specific for the protein NS4 of hepatitis C virus in patients with chronic hepatitis C. *J. Exp. Med.* 178, 17–25.

Nelson, P. J., Kim, H. T., Manning, W. C., Goralski, T. J., and Krensky, A. M. (1993). Genomic organization and transcriptional regulation of the RANTES chemokine gene. *J. Immunol.* 151, 2601–2612.

Nelson, P. J., Ortiz, B. D., Pattison, J. M., and Krensky, A. M. (1996). Identification of a novel regulatory region critical for expression of the RANTES chemokine in activated T lymphocytes. *J. Immunol.* 157, 1139–1148.

Nuti, S., Rosa, D., Valiante, N. M., Saletti, G., Caratozzolo, M., Dellabona, P., Barnaba, V., and Abrignani, S. (1998). Dynamics of intra-hepatic lymphocytes in chronic hepatitis C: Enrichment for Valpha24+ T cells and rapid elimination of effector cells by apoptosis. *Eur. J. Immunol.* 28, 3448–3455.

Pape, G. R., Gerlach, T. J., Diepolder, H. M., Gruner, N., Jung, M., and Santantonio, T. (1999). Role of the specific T-cell response for clearance and control of hepatitis C virus. *J. Viral Hepat.* 6(Suppl. 1), 36–40.

Peterson, K. E., Robertson, S. J., Portis, J. L., and Chesebro, B. (2001). Differences in cytokine and chemokine responses during neurological disease induced by polytropic murine retroviruses Map to separate regions of the viral envelope gene. *J. Virol.* 75, 2848–2856.

Polyak, S. J., Khabar, K. S., Paschal, D. M., Ezelle, H. J., Duverlie, G., Barber, G. N., Levy, D. E., Mukaida, N., Gretch, D. R. (2001). Hepatitis C virus nonstructural 5A protein induces interleukin-8, leading to partial inhibition of the interferon-induced antiviral response. *J. Virol.* 75, 6095–6106.

Sansonno, D., De Vita, S., Iacobelli, A. R., Cornacchiulo, V., Boiocchi, M., Dammacco, F. (1998). Clonal analysis of intrahepatic B cells from HCV-infected patients with and without mixed cryoglobulinemia. *J. Immunol.* 160, 3594–3601.

Schall, T. J. (1991). Biology of the RANTES/SIS cytokine family. *Cytokine* 3, 165–183.

Schall, T. J., Bacon, K., Toy, K. J., and Goeddel, D. V. (1990). Selective attraction of monocytes and T lymphocytes of the memory phenotype by cytokine RANTES. *Nature* 347, 669–671.

Selby, M. J., Choo, Q. L., Berger, K., Kuo, G., Glazer, E., Eckart, M., Lee, C., *et al.* (1993). Expression, identification and subcellular localisation of the proteins encoded by the hepatitis C viral genome. *J. Gen. Virol.* 74, 1103–1113.

Shimizu, Y. K., Purcell, R. H., and Yoshikura, H. (1993). Correlation between the infectivity of hepatitis C virus *in vivo* and its infectivity *in vitro*. *Proc. Natl. Acad. Sci. USA* 90, 6037–6041.

Shrivastava, A., Manna, S. K., Ray, R., and Aggarwal, B. B. (1998). Ectopic expression of hepatitis C virus core protein differentially regulates nuclear transcription factors. *J. Virol.* 72, 9722–9728.

Shyy, Y. J., Li, Y., and Kolattukudy, P. E. (1993). Activation of MCP-1 gene expression is mediated through multiple signaling pathways. *Biochem. Biophys. Res. Commun.* 192, 693–699.

Suzuki, R., Matsuura, Y., Suzuki, T., Ando, A., Chiba, J., Harada, S., Saito, I., and Miyamura, T. (1995). Nuclear localization of the truncated hepatitis C virus core protein with its hydrophobic C terminus deleted. *J. Gen. Virol.* 76, 53–61.

Tai, D. I., Tsai, S. L., Chen, Y. M., Chuang, Y. L., Peng, C. Y., Sheen, I. S., Yeh, C. T., Chang, K. S., Huang, S. N., Kuo, G. C., and Liaw, Y. F. (2000). Activation of nuclear factor kappaB in hepatitis C virus infection: Implications for pathogenesis and hepatocarcinogenesis. *Hepatology* 31, 656–664.

Taub, D. D., Sayers, T. J., Carter, C. R., and Ortaldo, J. R. (1995). Alpha and beta chemokines induce NK cell migration and enhance NK-mediated cytolysis. *J. Immunol.* 155, 3877–3888.

Tomei, L., Failla, C., Santolini, E., De-Francesco, R., and La-Monica, N. (1993). NS3 is a serine protease required for processing of hepatitis C virus polyprotein. *J. Virol.* 67, 4017–4026.

Tsai, S. L., and Huang, S. N. (1997). T cell mechanisms in the immu-

nopathogenesis of viral hepatitis B and C. *J. Gastroenterol. Hepatol.* **12,** S227–S235.

Tsai, S. L., Liaw, Y. F., Chen, M. H., Huang, C. Y., and Kuo, G. C. (1997). Detection of type 2-like T-helper cells in hepatitis C virus infection: Implications for hepatitis C virus chronicity. *Hepatology* **25,** 449–458.

Valiante, N. M., D'Andrea, A., Crotta, S., Lechner, F., Klenerman, P., Nuti, S., Wack, A., and Abrignani, S. (2000). Life, activation and death of intrahepatic lymphocytes in chronic hepatitis C. *Immunol. Rev.* **174,** 77–89.

Watashi, K., Hijikata, M., Marusawa, H., Doi, T., and Shimotohno, K. (2001). Cytoplasmic localization is important for transcription factor nuclear factor-kappa B activation by hepatitis C virus core protein through its amino terminal region. *Virology* **286,** 391–402.

Yoshida, H., Kato, N., Shiratori, Y., Otsuka, M., Maeda, S., Kato, J., and Omata, M. (2001). Hepatitis C virus core protein activates nuclear factor kappa B-dependent signaling through tumor necrosis factor receptor-associated factor. *J. Biol. Chem.* **276,** 16399–16405.

You, L. R., Chen, C. M., and Lee, Y. H. (1999). Hepatitis C virus core protein enhances NF-kappaB signal pathway triggering by lymphotoxin-beta receptor ligand and tumor necrosis factor alpha. *J. Virol.* **73,** 1672–1681.

Zehender, G., Meroni, L., De Maddalena, C., Varchetta, S., Monti, G., and Galli, M. (1997). Detection of hepatitis C virus RNA in CD19 peripheral blood mononuclear cells of chronically infected patients. *J. Infect. Dis.* **176,** 1209–1214.

Zheng, X. M., Wang, Y., and Pallen, C. J. (1992). Cell transformation and activation of pp60c-src by overexpression of a protein tyrosine phosphatase. *Nature* **359,** 336–339.